The Thesis Committee for Rachael Nichole Isphording
Certifies that this is the approved version of the following thesis:

Long-term Atmospheric Circulation Variability in the Tropics Linked to Climate Changes in the Amazon and Congo

APPROVED BY

SUPERVISING COMMITTEE:

Supervisor:

Robert Dickinson

Rong Fu, Cosupervisor

Zong-Liang Yang

Long-term Atmospheric Circulation Variability in the Tropics Linked to Climate Changes in the Amazon and Congo

by

Rachael Nichole Isphording

Thesis

Presented to the Faculty of the Graduate School of

The University of Texas at Austin

in Partial Fulfillment

of the Requirements

for the Degree of

Master of Science in Geological Sciences

The University of Texas at Austin

December 2017

Dedication

To my Grandma, Christine Isphording; she was the quintessence of kindness, benevolence, and magnanimity. Her love, strength and overwhelming optimism inspired me to always follow my heart, to never give up on myself or my dreams, and to always stay hopeful and sanguine in the most difficult and seemingly impossible situations. She is a paragon of the person I hope to become.

To Shawn Milrad; his unyielding and unconditional friendship and support were my backbone and lifeline throughout this ordeal. I have never had anyone I could rely on so illimitably, and I couldn't have gotten through the last two years without him.

To Brian Isphording, Elena Isphording, Brittany Isphording, Nick Mustin, Wayne Isphording, Marley Redditt, Shelley Arnold, Carey Anne Sikorowski, Rachel Britnell, Drew Ulmer, Brandon Saxon, Anje Williams, Lily Jackson, Natasha Sekhon, and John Li. Families are complicated and messy at times, but they are also beautiful. They are the people that you can depend on during your worst moments, and they are the people with whom you share your best moments. Thank you all for the reassurance, the support, the laughs, the tears, the conversations, and the arguments that got me through this. I am very lucky to be able to call you my family. Y'all gave me the strength to persevere through my many moments of self-doubt and adversity. Thank you.

To Mr. Willy and Mrs. Nancy Foster; they taught me at a very young age to work hard and follow my passion but to always remain humble, generous, and gracious. They also taught me that I don't have to be the best as long as I am the best that I can be.

To Dale Kaiser; his mentorship and encouragement has been profoundly influential in numerous ways on my journey to become a climate scientist. Thank you.

Acknowledgements

I would like to acknowledge and thank the following individuals without whose feedback and support this thesis would not have been possible.

I would first like to thank my advisor, Rong Fu. Her unwavering patience, empathy, encouragement, and mentorship allowed me to grow profoundly as both a scientist and a person throughout the completion of this thesis. I would also like to thank my committee members Robert Dickinson and Zong-Liang Yang whose guidance enhanced the quality of my research and my abilities as a scientist. I would also like to thank Muhammad Shaikh for his patience and assistance in continuously helping me to debug my code and his feedback as this project was first developed. I learned more and accomplished more in two years than I would have ever thought possible, and I am deeply grateful for the inspiration, encouragement, and guidance from these individuals.

I would also like to acknowledge the extensive and unrelenting help of Philip Guerrero, the Graduate Program Administrator. I would not have succeeded in this program without his support and advocacy. I would like to thank Lily Jackson, Natasha Sekhon, and John Li for their unrelenting support, friendship, and personal and intellectual advice throughout this process. I am very grateful for each of you.

Lastly, I would like to thank and acknowledge the professors of the Applied Meteorology Program at Embry-Riddle Aeronautical University for giving me a strong background in atmospheric science, always believing in my abilities as a scientist, and encouraging me to be my best. I would especially like to thank Dr. Shawn Milrad for his extensive feedback on the many drafts of this thesis as well as the countless hours he spent helping me interpret and design code for complex analyses.

Abstract

Long-term Atmospheric Circulation Variability in the Tropics Linked to Climate Changes in the Amazon and Congo

Rachael Nichole Isphording, M.S.

The University of Texas at Austin, 2017

Supervisors: Rong Fu and Robert Dickinson

Presently, there has not been an attempt to holistically understand regional manifestations of tropical atmospheric circulation systems or how long-term changes in these systems have influenced the climate in the Amazon or the Congo. This study provides insight into long-term (1900–2010) changes in the Hadley Circulation and Walker Circulation with a focus on connecting these tropical circulation changes to regional and seasonal climate change in the Amazon and Congo tropical forests. Based on the results of this study, it can be concluded that the Hadley Circulation has distinct regional manifestations and has not changed uniformly across different regions. Globally, the Hadley Circulation has strengthened in the Southern Hemisphere and weakened in the Northern Hemisphere for the 1900–2010 time period. However, the Hadley Circulation over the Amazon indicates strengthening in both hemispheres and weakening in both hemispheres over the Congo. A strengthening of the Walker Circulation has also been identified in the Pacific and Atlantic Ocean and over the Maritime Continent. However, long-term changes of the Walker Circulation over the Atlantic are indicative to Atlantic

Niño (Atlantic counterpart of the El Niño) conditions, as represented in substantial reversals of climatological zonal wind patterns. These wind reversals indicate less moisture influx into the Amazon from the Atlantic Ocean and more moisture influx into the Congo from the Atlantic although long-term precipitation trends indicate more drying in the Congo than the Amazon.

This study provides valuable insight into how interactions between oceans and atmospheric circulation systems influence regional climate in the Amazon and Congo as well as large-scale changes in the full tropical belt. These findings will help to improve climate projections in the tropics by providing an essential foundation of seasonal and regional manifestations of tropical atmospheric circulation systems and how long-term changes in these systems have influenced climate in the Amazon and the Congo forests.

Table of Contents

List of Tables

List of Figures

1. INTRODUCTION

1.1 Background

Earth's tropical forests are one of the planet's greatest natural treasures, providing habitat to an extraordinary diversity of species [*Betts et al.*, 2008; *Cusack et al.*, 2016], playing an essential role in the global carbon cycle and other biogeochemical processes [*Clark*, 2004; *Pan et al.,* 2011], and regulating local, regional, and global climate through atmospheric circulation feedbacks [*Werth and Avissar*, 2002; *Hilker et al.*, 2014]. It is well-established that tropical forests decrease surface temperatures through maintaining high rates of evapotranspiration and increase regional precipitation rates compared to other land surface types [*Bonan*, 2008]. Furthermore, tropical forests account for approximately 25% of the carbon stored in the terrestrial biosphere [*Bonan*, 2008] and dominate the exchange of carbon dioxide (CO_2) between the land and atmosphere in the carbon cycle [*Pan et al.*, 2011]. Ongoing deforestation has already released large amounts of CO_2 into the atmosphere, particularly in Brazil where Amazon deforestation stands as the country's largest source of CO_2 emissions [*Morton et al.*, 2006]. Potential degradation due to climate change threatens to vitiate these valuable terrestrial carbon sinks while simultaneously forcing their transition to a major carbon source [*Brienen et al.*, 2015] and enhancing regional and global warming through positive feedbacks to the climate system [*Bonan*, 2008; *Malhi et al.*, 2008; *Cusack et al.*, 2016]. Despite the unquestionable significance of these critical ecosystems and the breadth of current knowledge, there is still much uncertainty surrounding the complex forcings and feedbacks that drive change in tropical forests.

The Amazon and Congo Rainforests are the two largest, intact, global tropical forests; they account for roughly half of all global forested area and nearly 70% of the

global tropical forest area [*Pan et al.,* 2011]. As such, these ecosystems are critical to both global and regional climate systems and hold great socioeconomic value. Both the Amazon and Congo have experienced a significant increase in surface temperature. In recent decades, the Amazon and the Congo have witnessed a reduction in regional rainfall and multiple occasions of extreme drought conditions [*Malhi and Wright*, 2004; *Lewis et al.,* 2011; *Marengo et al.,* 2011; *Asefi-Najafabady and Saatchi*, 2013; *Fu et al.,* 2013; *Hua et al.,* 2016]. While these events appear attributable to natural climate variability [*Marengo et al.,* 2008], it is not clear whether anthropogenic climate change also exacerbates surface warming and droughts. Precipitation patterns in these regions are driven by complex interactions between the ocean, land surface/vegetation, and tropical atmospheric circulation systems (i.e., the Hadley Circulation and the Walker Circulation). To what degree the large-scale circulation change induced by global climate change can contribute to the observed rainfall change in the Amazon and the Congo has not been clearly addressed.

In the simplest terms, the Hadley and Walker Circulations are large-scale, overturning atmospheric circulation systems that are essential to regulating Earth's energy budget and hydrological cycle. As shown in Figure 1, the Hadley Circulation is centered at the equator where ascent and convection occur and extends out to the subtropics in both hemispheres (separately referred to as Hadley Cells) where subsidence and high pressure dominate. The Hadley Circulation is driven by meridional temperature gradients and transports surplus heat from the equator (region of maximum solar insolation) to the poles [*Webster*, 2004]. The Walker Circulation is characterized by low-level easterly winds and upper-level westerly winds over the Pacific and Atlantic Ocean; over the Indian Ocean, the Walker Circulation is characterized by low-level westerly flow and upper-level easterly flow. Convection due to the Walker Circulation occurs over

2

the Maritime Continent, equatorial South America, and to a much lesser degree equatorial West Africa. These climatological conditions of the Walker Circulation can also be seen in Figures 8A and 9A in which the climatological zonal winds and geopotential heights are plotted.
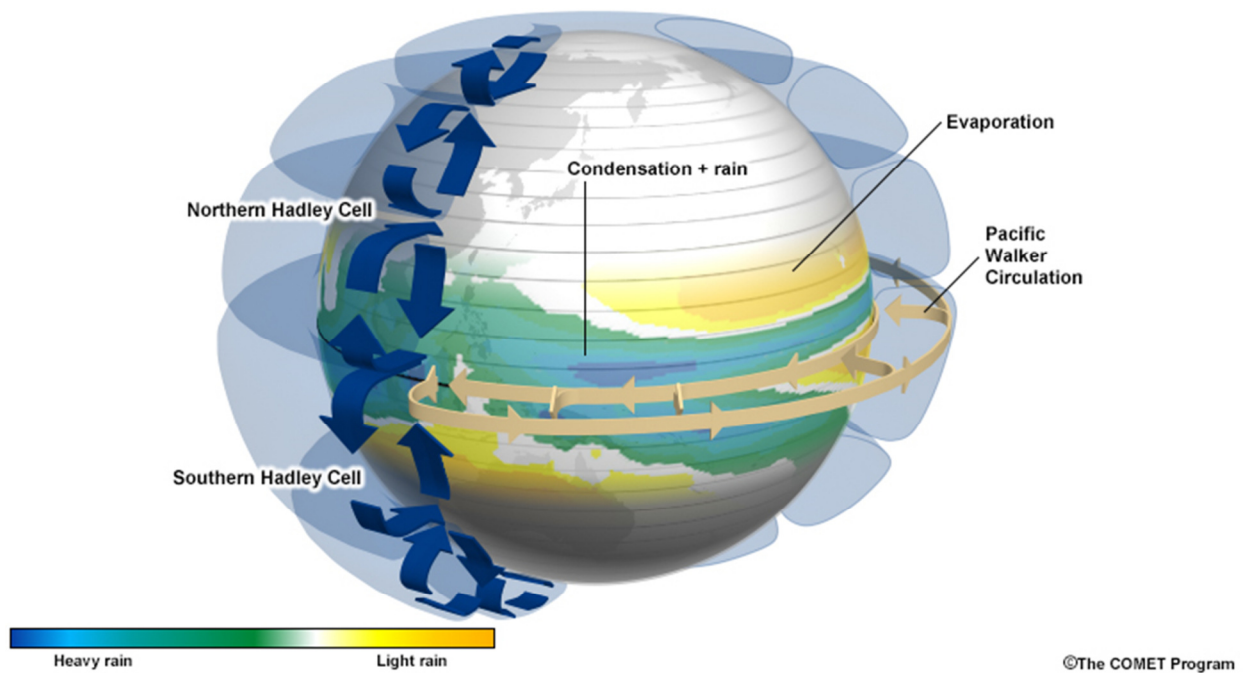
Figure 1:   Schematic diagram showing the idealized representation of the Hadley Circulation and Walker Circulation [*COMET MetEd*, 2015].

Both the Hadley Circulation and the Walker Circulation largely influence precipitation patterns in the tropics and subtropics and as such, the location of the planet's tropical forests and subtropical deserts. Earth's tropical forests are centered around the equator where ascent and deep convection occur, and global deserts persist in the subtropics where subsidence and high pressure from the Hadley Circulation dominate. Changes in the Hadley and Walker Circulations interrupt these prevailing precipitation patterns which can be significantly consequential for tropical/subtropical communities and ecosystems. Short-term variability of these tropical circulation systems can result in

severe droughts or floods that can be economically, politically, and environmentally deleterious. Prolonged variability can shift the location of global tropical rainforest and desert regions.

1.2 Motivation

Fluctuations in tropical atmospheric circulation systems have impacted human civilizations in the tropics for thousands of years. Evidence of contraction/expansion of the Hadley Cells is speculated to have determined settlement locations of ancient civilizations in the tropics [*Oslisly et al.*, 2013; *Carson et al.,* 2014] and potentially triggered the demise of some of these ancient civilizations [*Hodell et al.,* 1995]. Today, nearly half of the planet's population resides in the tropics [*Winter et al.,* 2015], almost all of whom are in developing countries that are at much higher risk from climate-driven, socioeconomic vulnerabilities. Limited resources, evolving management techniques, and poor infrastructure make these regions especially susceptible to climatic changes. Precipitation patterns, including extreme precipitation events, are particularly important for water resource management, agriculture, hydroelectric energy production, health, and infrastructure in these regions. Changes in the tropical atmospheric circulation systems— and therein changes in associated precipitation patterns—would hinder progress and exacerbate hardship in these countries [*Adger et al.*, 2003; *Mertz et al.,* 2009]. Creating effective risk mitigation strategies, development plans, and resource management plans would require an enhanced understanding of changes in the Hadley and Walker Circulations to improve climate projections and precipitation assessments in the tropics.

The productivity and the health of the Amazon and Congo are also threatened by changes in the Hadley and Walker Circulations. While there has been substantial research

investigating recent precipitation decline in these tropical forests as well as recent changes in the tropical atmospheric circulation systems, the two areas of focus remain largely disconnected. Studies assessing recent changes in the Hadley Circulation tend to focus on decadal, global change [*Hu and Fu*, 2007; *Lu et al.,* 2009; *Liu et al., 2012*], and studies evaluating recent changes in the Walker Circulation tend to focus on the response of the Walker Circulation to anthropogenic warming, particularly warming manifested in changing sea surface temperatures [*L'Heureux et al.,* 2013; *McGregor et al., 2014*]. Research into tropical forest precipitation patterns tends to focus on ocean interactions and localized influences [*Malhi and Wright*, 2004; *Lewis et al.,* 2011; *Asefi-Najafabady and Saatchi*, 2013; *Fu et al.,* 2013; *Hua et al.,* 2016]. Minimal studies have evaluated changes in the Walker Circulation or the Hadley Circulation in direct relation to climate changes in either the Amazon or the Congo. Furthermore, there has not been an attempt to holistically understand regional manifestations of tropical atmospheric circulation systems or how long-term changes in these systems have influenced the climate in the Amazon or the Congo. Because variations in the Hadley and Walker Circulations reflect changes in the magnitude and location of tropical warming [*Held and Hou*, 1980; *Horel and Wallace*, 1981; *Vecchi et al*., 2006; *L'Heureux et al.,* 2013], a deeper understanding of both regional and long-term fluctuations in these systems will provide valuable insight into complex interactions and feedbacks in the tropics.

1.3 Objectives

Although Abram et al. [2016] found that the onset of global warming occurred in the mid-1800s, extensive paleoclimate records indicate that only the twentieth century has witnessed warm extremes in both hemispheres in the last millennium [*Neukom et al.*,

2014]. That being said, this study focuses largely on the twentieth century but also includes the first decade of warming that took place in the twenty-first century. The overarching goal of this study is to provide insight into long-term (1900–2010) changes in the Hadley Circulation and Walker Circulation with a focus on connecting these tropical circulation changes to regional and seasonal climate change in the Amazon and Congo tropical forests. The main objectives are to:

1)   Determine how the Hadley Circulation is expressed regionally over the Amazon and Congo

2)   Identify long-term trends in the tropical circulation patterns seasonally, regionally and globally

3)   Infer the contribution of tropical circulation changes to observed precipitation changes in the Amazon and Congo

4)   Determine the extent to which individual ocean basin warming in the Pacific, Atlantic, and Indian Oceans influence tropical circulation changes and precipitation patterns in the Amazon and Congo

2. DATA AND METHODS

2.1 Data

The results and conclusions of this study are based on gridded reanalysis data that provide reliable temporal coverage during the 20th century and early 21st century (i.e., 1900–2010). Furthermore, datasets were chosen that provided ample spatial coverage over the Amazon and Congo for the full time period. Datasets and variable specifications used in this study are summarized in Table 1 below.

Data Set	Reference	Variable	Resolution
GPCC	*Schneider et al.*, 2014	Precipitation	0.5°x0.5°, 1901–2010, Monthly totals
CRU TS 3.23	*Harris et al.*, 2014	Precipitation	0.5°x0.5°, 1901–2010, Monthly totals
ERSST.v4	*Huang et al.,* 2015	Sea surface temperature	2°x2°, 1901–2010, Monthly mean
ERA-20CM	*Hersbach et al.*, 2013	Surface Pressure Geopotential height Zonal wind Meridional wind	0.5°x0.5°, 1900–2010, Monthly mean

Table 1: Summary of reanalysis data evaluated in this study.

The primary precipitation dataset used in this study is the Global Precipitation Climatology Centre (GPCC) gridded dataset [*Rudolf and Schneider*, 2005; *Becker et al.,* 2013; *Schneider et al*. 2014]. GPCC is widely accepted as the most reliable and consistent source of long-term global precipitation data as it assimilates the largest number of quality controlled, gauge-based observations with more than 67,000 stations worldwide [*Schneider et al.,* 2014; *Soares et al.*, 2016]. Furthermore, Juarez et al. [2009] found that GPCC precipitation data agrees with several other precipitation datasets (over tropical South America). There is less agreement between other precipitation datasets over the Congo [*Juarez et al.,* 2009], but this can be expected as ongoing civil conflicts,

disjointed politics, and infrastructure challenges in this region limit the ability to collect reliable, long-term station observations. For this reason, it should be noted that GPCC analyses over the Amazon are more reliable than those over the Congo. However, GPCC still provides the most spatial coverage over the Amazon and Congo during the 20th century, justifying its use as the main precipitation dataset. GPCC data was compared to the Climatic Research Unit Time Series Version 3.23 (CRU TS 3.23) dataset [*Harris et al.*, 2014] as it is the only other long-term, observation based dataset that provided ample spatial coverage over both the Amazon and Congo during the 20th century. Both the GPCC and CRU TS 3.23 provide monthly precipitation totals on a 0.5° x 0.5° grid starting from 1901 and ending after 2010, allowing for easy comparison. The sea surface temperature (SST) dataset used in this study is the NOAA Extended Reconstructed Sea Surface Temperature Version 4 (ERSST.v4) [*Huang et. al.,* 2015). ERSST.v4 provides monthly mean SST data dating back to 1854 on a 2° x 2° grid and is accepted as a reliable, long-term dataset for global SSTs [*Huang et. al.,* 2015]. Furthermore, it is regarded as the most unbiased global SST dataset that most closely matches measurements from independent, instrumentally uniform measurements from near-global floating buoys; it is has also been found to most accurately capture SSTs during the debated global warming hiatus of the early 21st century [*Hausfather et al.,* 2017].

Finally, the European Centre for Medium-range Weather Forecasts's (ECMWF) 20th Century Reanalysis Model Ensemble (ERA-20CM) dataset was used for three-dimensional atmospheric fields [*Hersbach et al.,* 2013]. ERA-20CM has a horizontal resolution of 0.5° x 0.5°, 91 vertical levels, and is available on a global grid from 1900–2010. ERA-20CM has been shown to be reliable for diagnostics and statistical estimates of the climate and climatic trends during the 20th century [*Hersbach et al.,* 2013]. Furthermore, utilizing this reanalysis dataset allows for a comparison to long-term trends

identified in the Hadley Circulation using the NCEP 20th Century Reanalysis Version 2 (20CR2) dataset in a study by Liu et al. [2012]. Monthly means of atmospheric fields examined in this study include: surface pressure, geopotential height, and zonal and meridional wind components. Finally, all figures and plots were created using NCAR's Command Language (NCL) version 6.3.0.

2.2 Methods

2.2.1 ANOMALIES OF VARIABLE FIELDS

A base climatology of 1971–2000 was used to calculate the anomalies of each variable field; this base climatology was used as to not include major warming that occurred in the first decade of the twenty-first century. Seasonal anomalies were calculated for terrestrial precipitation over the Amazon (30°S–10°N, 80°–30°W) and the Congo (20°S–15°N, 20°W–50°E), SSTs within the tropical band (30°S–30°N), and the zonal wind at 850 hPa and 200 hPa within the tropics. Standardized seasonal and annual anomalies of the geopotential height at 850 hPa and 200 hPa were calculated within the tropics as well. The least-squares linear trend was calculated for geopotential height and zonal wind anomalies at 850 hPa and 200 hPa over the tropics for the entire 1900–2010 time period to deduce the degree and direction of long-term changes in both the Walker Circulation and Hadley Circulation, as discussed in further detail in the next chapter.

2.2.2 MERIDIONAL MASS STREAM FUNCTION

To evaluate regional and seasonal changes specifically in the Hadley Circulation, the meridional mass stream function (MMSF) was calculated. The MMSF is a standard way of representing the Hadley Circulation as it can be easily interpreted as a two-dimensional tracer of mass transport in the troposphere. The MMSF is defined as:

$$\psi = \frac{2\pi a\cos\varphi}{g} \int_0^p \bar{v}\,dp$$

where ψ represents the MMSF, α is the Earth's equatorial radius (6378 km), φ is the latitude, g is gravity (9.81 m s^{-2}), p is the pressure level, and $\bar{v}$ is the zonally-averaged meridional (north-south) wind. The MMSF at any given latitude and pressure level is equivalent to the rate at which air is transported meridionally between the given pressure level and the top of the atmosphere. The top of the atmosphere in this study was defined as 100 hPa. The regional Hadley Circulation over the Amazon and Congo was calculated by constraining the longitudinal bounds over which the meridional wind was zonally averaged. The Hadley Circulation over the Amazon was constrained to longitudinal boundaries of 80–45°W, and the Hadley Circulation over the Congo was constrained to longitudinal boundaries of 20°W–50°E. These longitudinal boundaries were selected to maximize the representation of the Hadley Circulation over the land surface and minimize the representation of the surrounding oceans. To further investigate long-term changes in the strength of the Hadley Circulation, the minimum and maximum values of the MMSF were extracted and the time series was plotted, similar to the methodology used in Liu et al. [2012]. The minimum value can be interpreted as the strength of the southern branch of the Hadley Circulation, and the maximum value can be interpreted as the strength of the northern branch of the Hadley Circulation.

2.2.3 EMPIRICAL ORTHOGONAL FUNCTIONS

Ocean basins are essential to the global energy budget and act as a major heat reservoir; since the 1950s, oceans have absorbed more than 90% of the total global energy surplus [*Levitus et al.*, 2012]. For this reason, ocean basin surface warming can be used as a crude proxy to anthropogenic warming. However, the warming of SSTs over

10

global oceans depends on ocean circulation and ocean-atmosphere interactions; the patterns of SST trends have a strong influence on the atmospheric circulation response and surface temperature and precipitation trends over Amazonia and the Congo [*Ma and Yu,* 2014; *McGregor et al.,* 2014; *He and Soden,* 2015]. Thus, it is important to also evaluate how warming SSTs influence long-term changes in tropical circulation systems on a regional and global scale. To accomplish this, empirical orthogonal functions (EOFs) were used to identify the warming pattern in each ocean basin's SSTs. The EOF is a statistical method used to identify the patterns that represent the maximum amount of variance in a particular data field as efficiently as possible. For this reason, it is frequently used in climate studies to objectively identify leading patterns of climate variability both spatially and temporally [*Lorenz*, 1956]. The first three EOF modes were calculated using the tropical (30°S–30°N) Atlantic Ocean (70°W–20°E), Pacific Ocean (120°E–70°W), and Indian Ocean (20°–120°E) SST anomalies separately and for each season. Each ocean basin and seasonal EOF modes were then tested for statistical significance in accordance with methods outlined in North et al. [1982] to confirm that each EOF was significantly different from the others. Upon confirming the statistical significance, each seasonal ocean basin warming mode (OBWM) was objectively identified as the leading EOF pattern that displayed a gradual warming trend. This was indisputably the first EOF mode for all seasons and ocean basins except for the Pacific Ocean during DJF and SON which captured El Niño patterns as the leading EOF mode. The second EOF mode was used as the OBWM for the Pacific Ocean during DJF and SON. The spatial and temporal representations of the OBWMs are shown in Figure 2.

2.2.4 DATASET RECONSTRUCTIONS

       In order to determine the degree to which each seasonal OBWM influenced long-term changes in tropical atmospheric circulation patterns and regional climate over the Amazon and Congo, select variable fields were reconstructed based on the seasonal OBWMs. The variable fields that were reconstructed include: regional precipitation anomalies over the Amazon and Congo, standardized geopotential height anomalies at
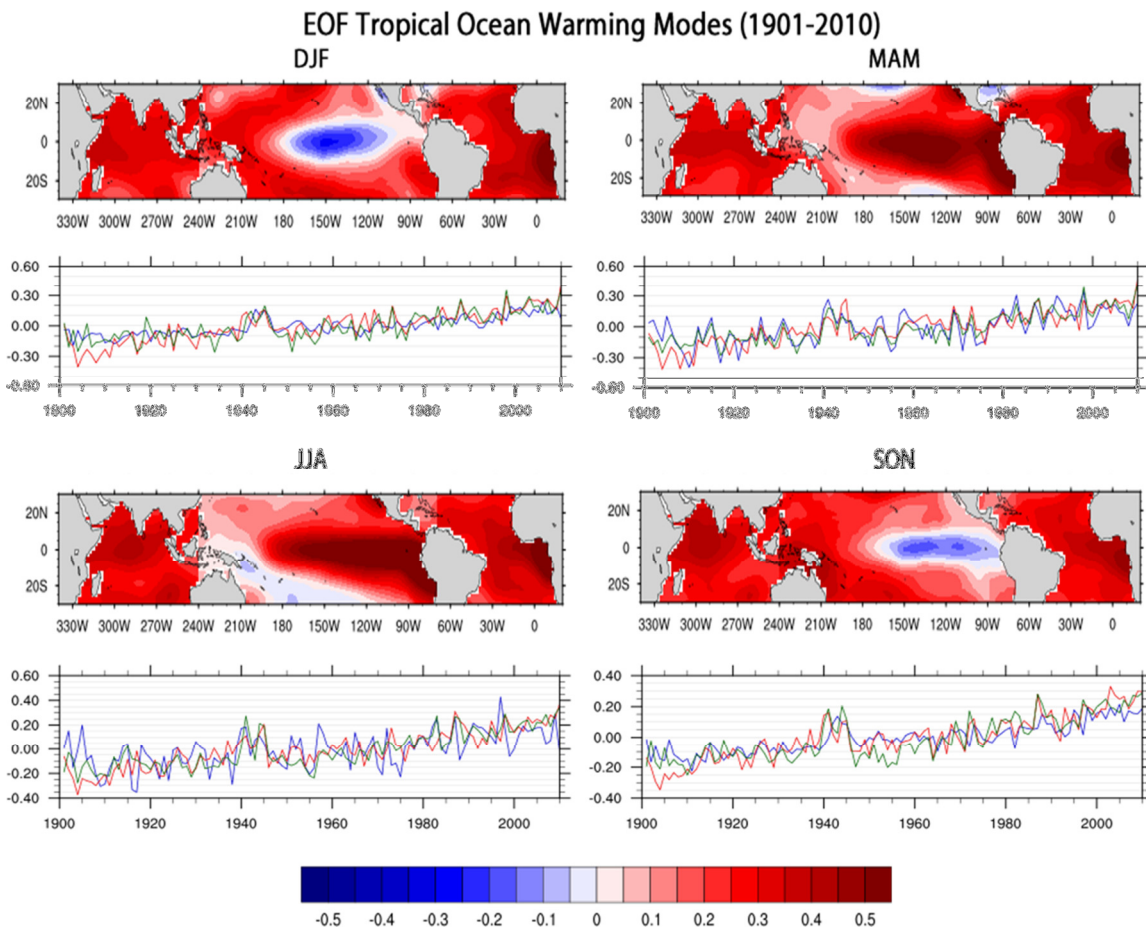
Figure 2:   Compiled OBWM scaled to °C. Contour maps indicate the degree spatial warming, and time series indicate the pattern of temporal warming where the blue line represents the Pacific Ocean, the red line represents the Atlantic Ocean, and the green line represents the Indian Ocean.

850 hPa and 200 hPa for the entire tropical belt, and zonal wind anomalies at 850 hPa and 200 hPa for the tropics. Reconstructing these three variable fields allows for substantial interpretation as to how tropical circulation and regional climate in the Amazon and Congo are influenced by ocean basin warming.

In order to calculate the reconstructed data, the seasonal anomaly of each variable field was first regressed against each seasonal OBWM time series (Fig. 2) at each grid point using least squares linear regression. The regression coefficient calculated at each grid point was then multiplied by the corresponding seasonal OBWM time series. The least squares linear trend was then calculated and plotted for seasonal reconstructions of the geopotential heights and zonal winds at 850 hPa (Fig. 11) and 200 hPa (Fig. 10) to show the degree to which ocean warming has influenced these variable fields over the past 110 years. These plots only include points which are significant according to methods outlined in Chen [1982] and Livezey and Chen [1983]. To determine the effective number of independent samples, the effective time of autocorrelation between each OBWM time series and variable field at each grid point was calculated using:

$$\tau = \left(1 + 2\sum_{i=1}^{N} C_{uu}(i\Delta t)C_{pp}(i\Delta t)\right)(\Delta t)$$

where $C_{uu}(i\Delta t)$ is the autocorrelation of the first time series (each respective OBWM), $C_{pp}(i\Delta t)$ is the autocorrelation of the second time series (the variable field at each grid point), $i\Delta t$ is the lag of the autocorrelation, Δt is the time step, and N is the number of samples. The effective time of autocorrelation (τ) was then used to calculate the effective number of independent samples for which to test the significance using the Student's t-test. The effective number of independent samples was calculated using:

$$n = \frac{N\Delta t}{\tau}$$

where the variables used match those explained above [*Chen,* 1982; *Livezey and Chen*, 1983].

The nonparametric Theil-Sen estimate of the linear trend was calculated for the reconstructed precipitation data over the Amazon and Congo and tested for significance using a two-sided Mann-Kendall trend test. The Theil-Sen trend estimator is insensitive to outliers and is defined as the median slope between all pairs of data [*Wilcox*, 2012]. It is robust to outliers and can be significantly more accurate than simple linear regression, particularly for skewed or non-Gaussian data [*Wilcox*, 2012]. The Mann-Kendall trend significance test was used to determine if the Theil-Sen trend was significantly increasing, decreasing, or monotonic.

3. RESULTS AND DISCUSSION

This section presents and discusses the results of the analyses of long-term changes in tropical circulation patterns and potential implications to regional climate changes over the Amazon and Congo tropical forests. First, there is a discussion of the regional manifestations of the Hadley Circulation over the full tropical belt, the Amazon and the Congo, respectively, based on the MMSF. Then, long-term, annual changes in the Hadley Circulation (using the MMSF) over the full tropics, Amazon, and Congo are discussed, followed by an overview of the long-term, seasonal changes in the Hadley Circulation over each region. The long-term trends of the overall changes in tropical atmospheric circulation are then discussed based on the geopotential heights and the winds at 200 hPa and 850 hPa followed by a discussion of the results of the trends of the variable fields reconstructed against each ocean basin warming mode. This discussion enhances the earlier analyses of the Hadley Circulation based on the MMSF and provides insight into long-term changes in the Walker Circulation and general climate change in the tropics. Furthermore, this allows for a preliminary analysis of the role individual ocean basin warming has played in long-term climate changes in the Amazon and Congo forests respectively as well as the full tropical belt. The limitations of the results are discussed in detail in the following chapter.

3.1 Interpretation of the Meridional Mass Stream Function

3.1.1 REGIONAL MANIFESTATIONS

The Hadley Circulation has distinct regional and seasonal characteristics that have not changed uniformly during the 1900–2010 analysis period. Based on the annual and seasonal climatology of the Hadley Circulation over the Amazon, Congo, and the entire

15

Figure 3: Annual and seasonal climatology (1971–2000) of the meridional mass stream function of the Hadley Circulation ($\times 10^{10}$ kg s^{-1}). The first column represents the stream function averaged over the entire tropical belt; the second column represents the stream function averaged over the Amazon (longitudinal boundaries of 80–45°W); the third column represents the stream function averaged over the Congo (longitudinal boundaries of 20°E–50°W).

16

tropical belt, respectively (Fig. 3), it is obvious that the Hadley Circulation has very diverse regional expressions. The annual and seasonal climatologies of the Hadley Circulation over the entire tropical belt agrees with previous studies, showing seasonally invariant overturning Hadley Cells mirrored around the equator and extending to the subtropics [*Dima and Wallace,* 2003]. During solstitial seasons, the Hadley Circulation is characterized by a strong, seasonally reversing, cross-equatorial cell with ascent in the outer tropics of the summer hemisphere and subsidence in the outer tropics of the winter hemisphere, as was also observed in Dima and Wallace [2003].

Based on the annual climatology (Fig. 3), the regional Hadley Circulation over the Congo exhibits much stronger, more defined, and more uniform Hadley Cells in both hemispheres than what is seen over the Amazon or the full tropical belt. The regional Hadley Circulation over the Congo also extends beyond 30° N/S which traditionally marks the bounding edges of the Hadley Circulation (as can be seen in the annual climatology for the full Tropics). In contrast, the annual climatology of the regional Hadley Circulation over the Amazon sector exhibits a very weak northern cell that only spans 10° in latitude. The northern regional Ferrel Cell intrudes far into the Tropics (to approximately 10°N) which indicates weaker uplift of the rising branch of the regional Hadley Circulation and a much stronger interaction with mid-latitude westerlies and associated transient baroclinic waves, as described by Webster [2004]. The regional southern branch over the Amazon is wider and stronger (based on the minimum value of the meridional mass stream function in Fig. 3), but it is also much shallower than the regional northern branch.

The regional Hadley Circulation over the Congo shows much greater seasonal homogeneity compared to that over the Amazon or the entire tropical belt (Fig. 3). Two strong, well-defined Hadley Cells are visible year-round over the Congo and are

predominantly stationary. However, the Congo Rainforest—which spans roughly 10°S–5°N—has a very distinct influence on the regional atmospheric circulation, particularly during the wet-to-dry transition season in JJA [*Zhou et al.,* 2014]. During JJA, the Congo rainforest is essentially engulfed by a "mini-circulation dome" within the boundary layer that is independent from the large-scale regional circulation system (Fig. 3). This "dome" is present in all seasons at varying magnitudes except DJF. However, there is a seasonally invariant "tail" that protrudes from the southern branch of the regional Hadley Circulation and surrounds the Congo rainforest. The Amazon rainforest—which spans roughly 15°S–10°N—shows far less influence over the regional Hadley Circulation (Fig. 3). Both branches of the regional Hadley Circulation over the Amazon migrate and intensify/weaken seasonally in a way that is analogous to the global mean Hadley Circulation. The regional northern branch is strongest over the Amazon during the Amazon's rainy season (DJF) which is also when the regional Ferrel Cell extends farthest into the Tropics and intensifies; this can most likely be attributed to an equatorward meandering of the mid-latitude westerly jet during the Northern Hemisphere winter.

The overall differences in both the annual and seasonal climatology of the regional Hadley Circulation over the Amazon and Congo, respectively, can largely be explained by the surface features surrounding both regions. The Congo is bordered by the world's largest non-polar desert (the Sahara) to the north and the Kalahari Desert to the south; the Amazon is bordered by the Caribbean Sea and Atlantic Ocean to the north and woody savannas and grasslands to the south. Since the Hadley Circulation is predominantly driven by meridional temperature gradients, the differential heating across land and sea is reflected in the regional expressions of the Hadley Circulation.
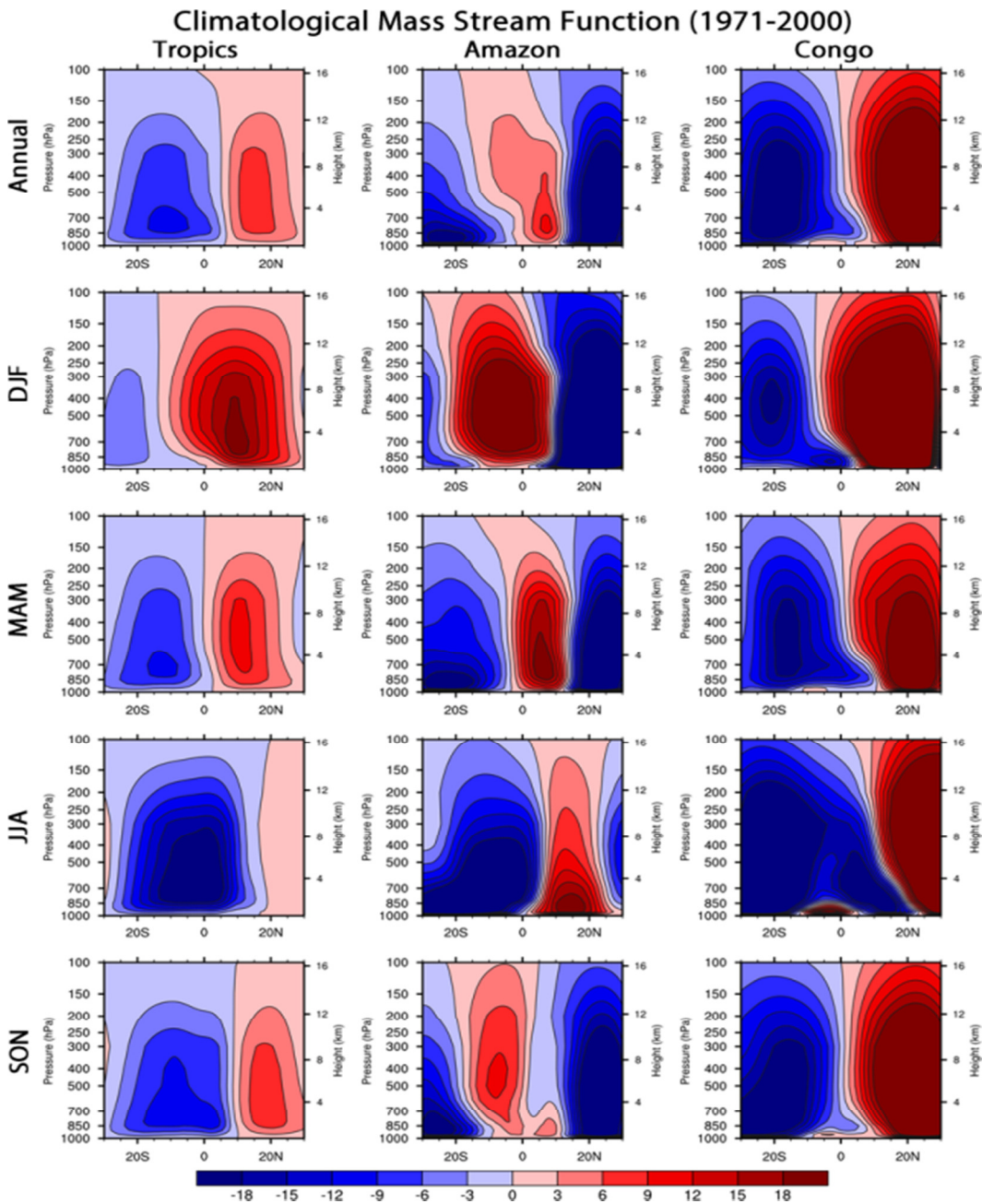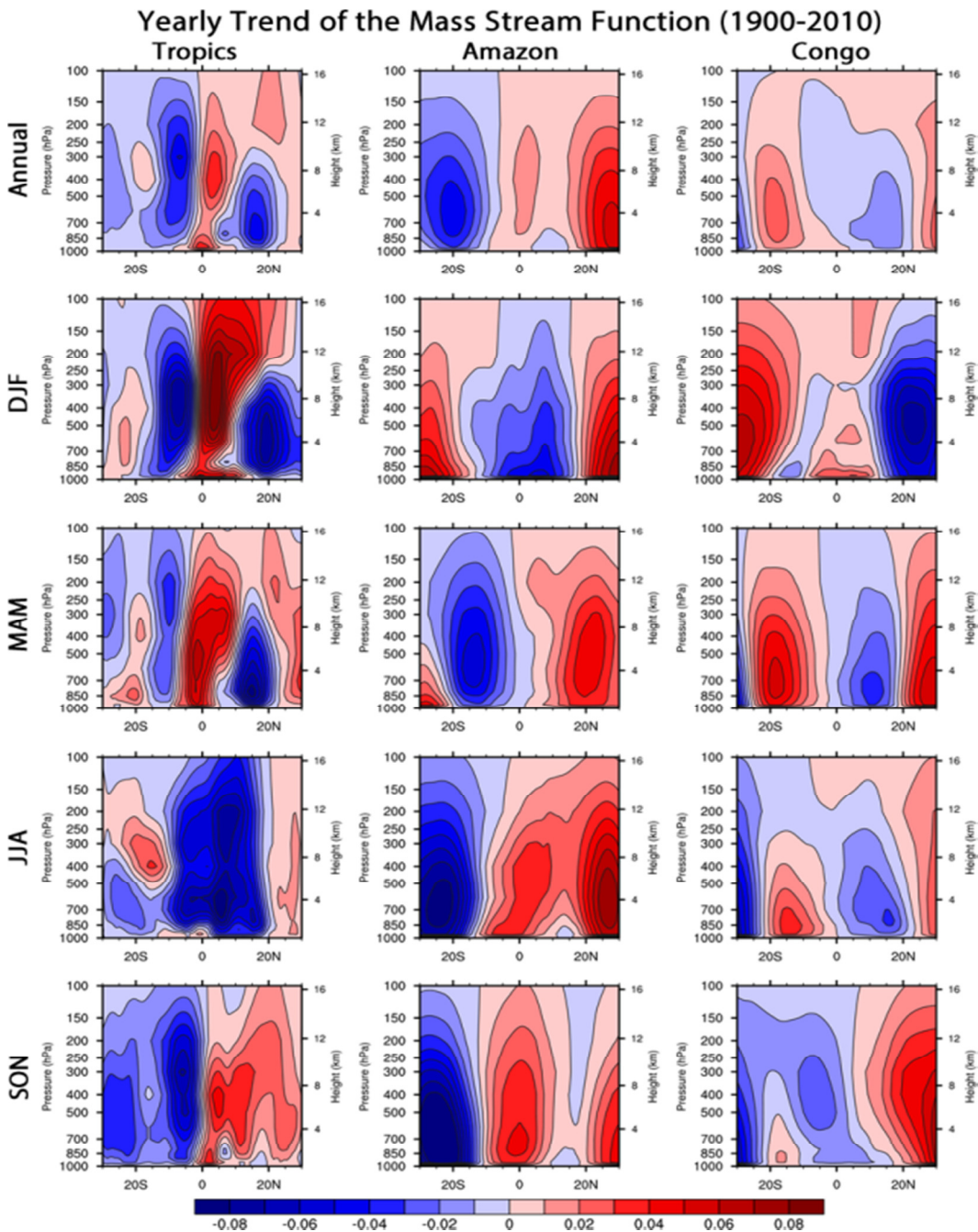
Figure 4:   Annual and seasonal linear trend (1971–2000) of the meridional mass
             stream function of the Hadley Circulation ($\times 10^{10}$ kg s^{-1} per year) over the
             entire tropical belt, the Amazon longitudinal boundaries, and the Congo
             longitudinal boundaries.

Decadal Trend of the Mass Stream Function (1900-2010)
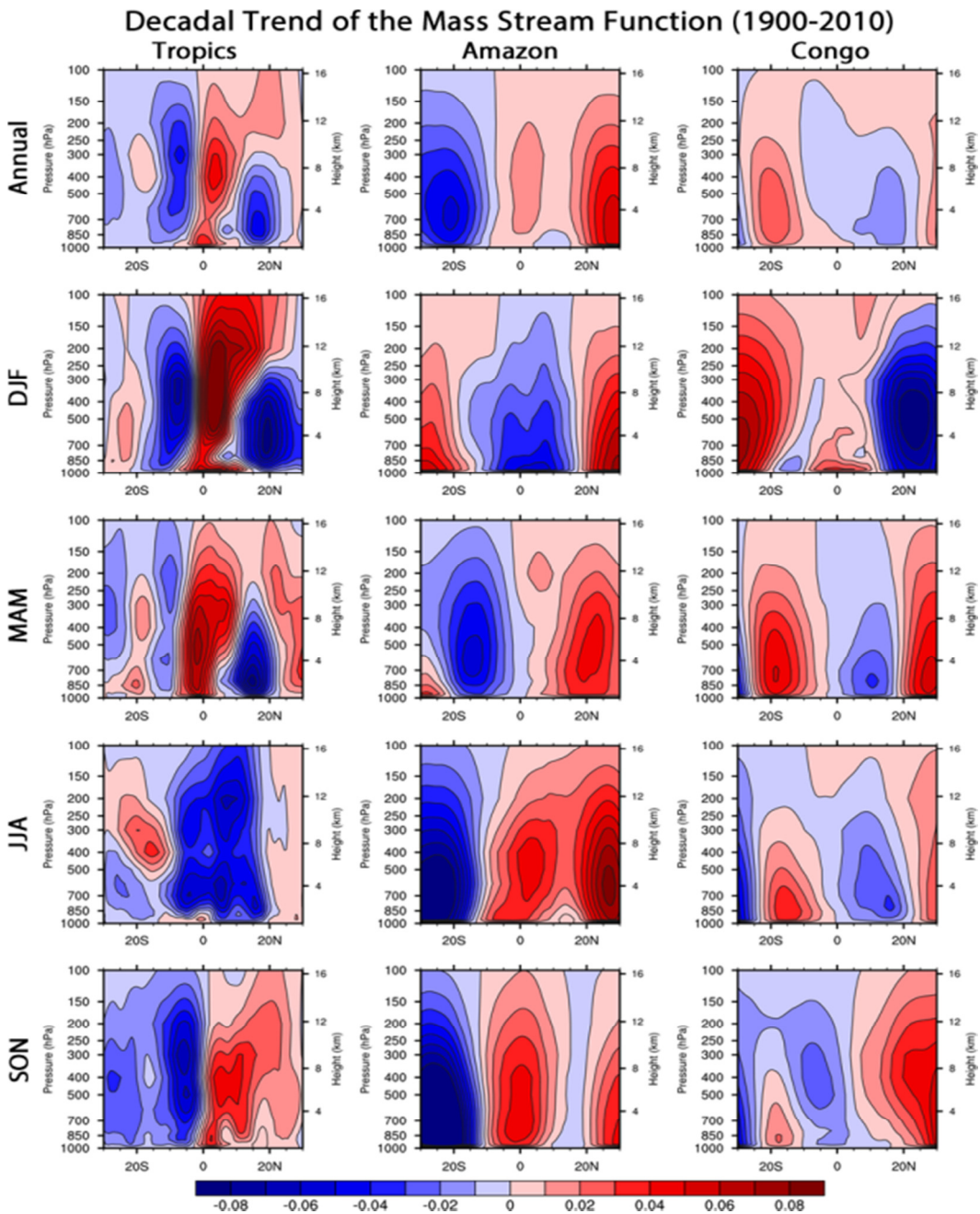
Figure 5: Annual and seasonal decadal linear trend (1971–2000) of the meridional mass stream function of the Hadley Circulation ($\times$ 10^{10} kg s^{-1} per decade) over the entire tropical belt, the Amazon longitudinal boundaries, and the Congo longitudinal boundaries.

3.1.2 LONG-TERM, ANNUAL TRENDS

The annual long-term trend of the Hadley Circulation varies widely between the full tropical belt, the Amazon, and the Congo as seen in Figures 4 and 5. The differences between the long-term yearly trends (Fig. 4) and the decadal trends (Fig. 5) of the regional and seasonal Hadley Circulation are minimal; this reinforces the robustness of the annual trends in Figure 4.

Using CMIP5 model projections, Lau and Kim [2015] suggested that greenhouse warming would result in a strengthening of the Hadley Circulation expressed in a narrowing and deepening of equatorial convection, enhanced uplift, and an expansion of the descending branches of the Hadley Circulation into the tropics and subtropics that would increase global dryness. Based on both the yearly trend (Fig. 4) and decadal trend (Fig. 5), long-term variation in the Hadley Circulation over the full tropical belt strongly resembles the "deep-tropics squeeze" observed in Lau and Kim [2015]. However, seasonal trends (Figs. 4 and 5) suggest that the deep-tropics squeeze is dominated by seasonal changes that occur during MAM and DJF. Furthermore, it appears that during 1900–2010, the deep tropics squeeze has been maximized in the Southern Hemisphere but stronger and wider subsidence has occurred in the Northern Hemisphere. This is also reflected in the time series of the strength of each Hadley Cell plotted in Figure 6 and 7; the northern branch of the annual Hadley Circulation shows a substantially stronger weakening trend over the tropics (Fig. 7) while the southern branch shows a slight strengthening from 1900–2010 (Fig. 6).

These results slightly contradict findings from previous studies evaluating the long-term trend in the strength and manifestation of the Hadley Circulation using other 20th century reanalysis datasets although the disagreement can largely be attributed to the length of time evaluated. Results based on the NCEP 20th Century Reanalysis Version 2

(20CR2) dataset that evaluate changes in the Hadley Circulation since 1871 [*Liu et al.,* 2012] demonstrate a similar long-term transition of the Hadley Circulation to a deep-tropics squeeze. Liu et al. [2012] observed a long-term contraction, deepening, and intensification along the equator although the magnitude of change in the Northern Hemisphere is much weaker than this study (Fig. 5). They observed similar long-term strengthening in the Southern Hemisphere (Figs. 5 and 6) but also saw large-scale strengthening in the Northern Hemisphere that contradicts with this study (Figs. 5 and 7). However, the Northern Hemisphere strengthening can most likely be attributed to a substantially weaker northern component of the Hadley Circulation that spans from 1871 to approximately 1900 [*Liu et al.,* 2012]. When this 30-year period is removed, the long-term trend in the strength of the northern component (Fig. 7) coincides with previous findings [*Liu et al.,* 2012] and indicates slight weakening since 1900.

Although the long-term trend in the Hadley Circulation over the tropical belt closely resembles the deep-tropics squeeze described by Lau and Kim [2015], regional long-term changes over the Amazon and Congo are not as directly supportive of this theory. Over the Amazon, the annual trend indicates a slight strengthening of the regional northern rising branch over the equator as well as an obvious expansion of the regional Northern Hemisphere Hadley Cell indicated by a profound weakening of the regional Ferrel Cell into the subtropics (Fig. 4 and 5). A deepening and narrowing of the regional southern rising branch is also observed in the annual trend although it is not fully obvious if the southern Hadley Cell is expanding or contracting. Another interesting feature in the annual long-term trend over the Amazon suggests enhanced localized moisture flow into the northern Amazon from the Atlantic Ocean and Caribbean Sea. The weakening of the regional, annual meridional mass stream function between 5–15°N in the lower

troposphere (Figs. 4 and 5) could indicate a strengthening of localized seabreezes due to greater warming of the land surface compared to the surrounding sea.

Over the Congo, both Hadley Cells show long-term weakening between 10–20° latitude, slight weakening of the rising northern branch, and strengthening in the rising southern branch between 25–30° latitude. The weakening that is present in the mid-tropics combined with weakening of lesser magnitude in the region of ascent and convection could indicate the long-term transition of the Hadley Circulation from its climatological manifestation (Fig. 3) into one that resembles the deep-tropics squeeze, although this deduction is rather speculative and far-reaching. Although the Congo rainforest shows a distinct presence in the climatological Hadley Circulation (Fig. 3), there doesn't appear to be any direct influence from the Congo in the long-term annual trend of variability in the regional Hadley Circulation (Figs. 4 and 5). This could be due to deforestation or long-term drying reducing the potential rate of evapotranspiration and other significant properties that impact the large-scale regional circulation [*Nogherotto et al.,* 2013; *Zhou et al.,* 2014]. Warming in the Pacific, Atlantic, and Indian Oceans all appear to be related to long-term regional drying (Fig. 19) and warming (Figs. 16–18) in the Congo forest, so global warming could also be responsible.

3.1.3 LONG-TERM, SEASONAL TRENDS

As previously stated, the annual trend over the full tropics predominantly reflects the combined seasonal changes during DJF and MAM. The intensification, deepening and contraction of the ascending branches of both cells of the Hadley Circulation are maximized in DJF over the full tropics (Figs. 4 and 5). This is also when the most substantial weakening of the northern Hadley Cell in the mid-to-low troposphere of the

23

Figure 6: Time series of the annual and seasonal mean (grey line) and the 10-year running mean (black line) of the strength of the southern component of the Hadley Circulation over the entire tropical belt, the Amazon longitudinal boundaries, and the Congo longitudinal boundaries.
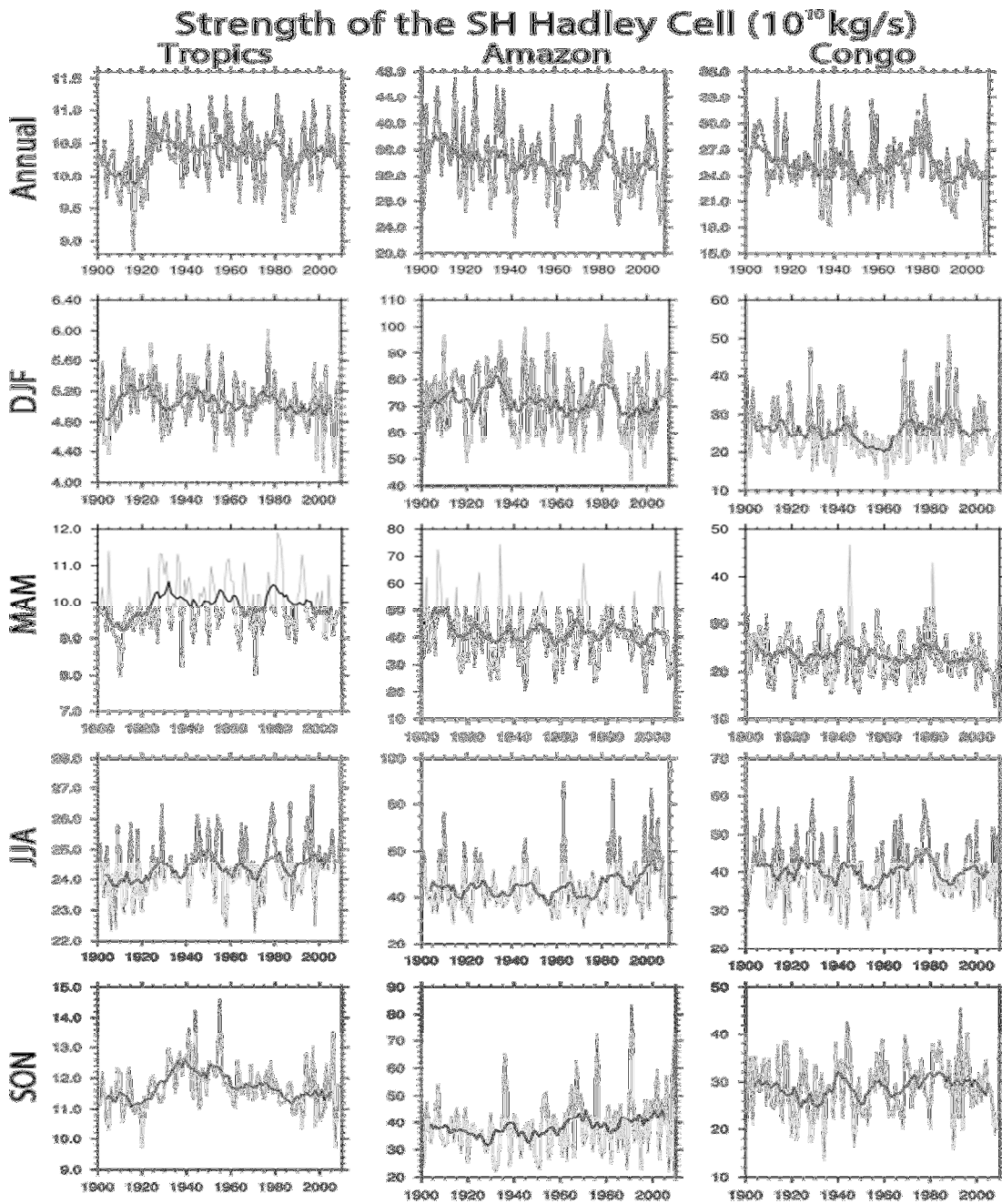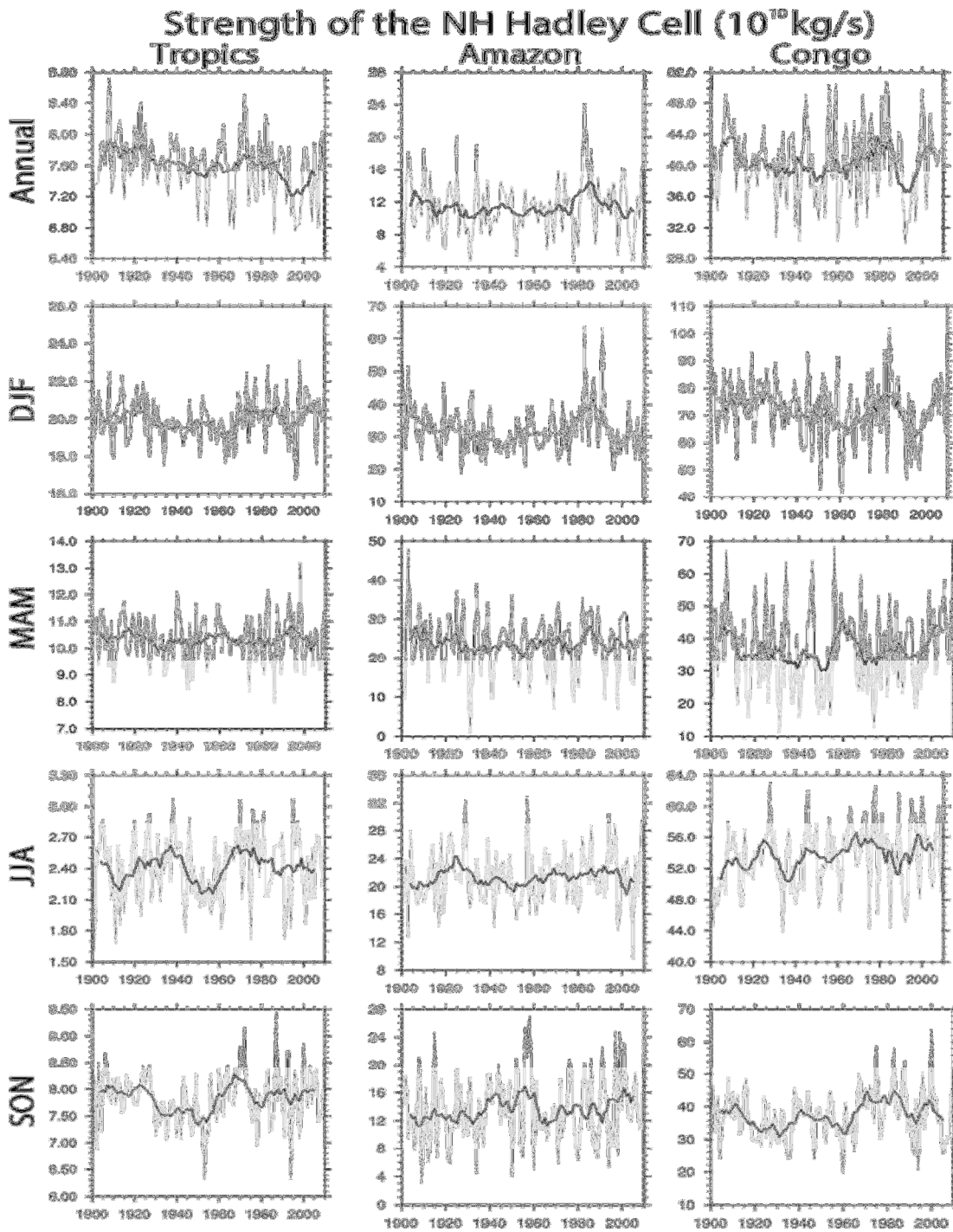
Figure 7: Time series of the annual and seasonal mean (grey line) and the 10-year running mean (black line) of the strength of the northern component of the Hadley Circulation over the entire tropical belt, the Amazon longitudinal boundaries, and the Congo longitudinal boundaries.

25

outer tropics occurs as well as the most uniform weakening of the southern Hadley Cell in this region. During MAM, there is also strong evidence of the deep-tropics squeeze, as well as potential strengthening and expansion of subtropical subsidence. However, it also appears that the sizable weakening that occurs during DJF in the Northern Hemisphere mid-to-low troposphere contracts and shifts slightly southward—concurrent with a slight southward migration of the Northern Hemisphere ascending branch—during MAM. The southern component of the Hadley Circulation averaged over the full tropics has intensified and deepened during JJA since 1900 (Figs. 4, 5, and 6). It also appears that the southern subtropical jet has tended to migrate equatorward during JJA since 1900 (Figs. 4 and 5), which has been attributed to regional drying in the Amazon [*Fu et al.,* 2013]. The long-term trend over the full tropics during SON further demonstrates intensification and narrowing of the ascending branches of the Hadley Circulation as well as expansion and intensification of subtropical subsidence (Figs. 4 and 5). However, it seems as though the strengthening of the Hadley Circulation is very much spatially dependent as the overall strength measured by the minimum/maximum values of the stream function do not show any discernable long-term trend since 1900 (Figs. 6 and 7).

The regional Hadley Circulation over the Amazon shows strongest overall weakening during DJF, the local rainy season (Figs 4–7). There is also an expansion of the northern regional Hadley Cell that decreases the presence of the regional Ferrel Cell into the subtropics. This long-term weakening and expansion during the rainy season could contribute to the regional reductions in rainfall that have occurred recently in the Amazon [*Malhi and Wright*, 2004; *Fu et al.*, 2013]. During MAM, the regional northern component expands, deepens, and strengthens while the regional southern component appears to contract, deepen, and intensify only between 5–20°S; these long-term trends
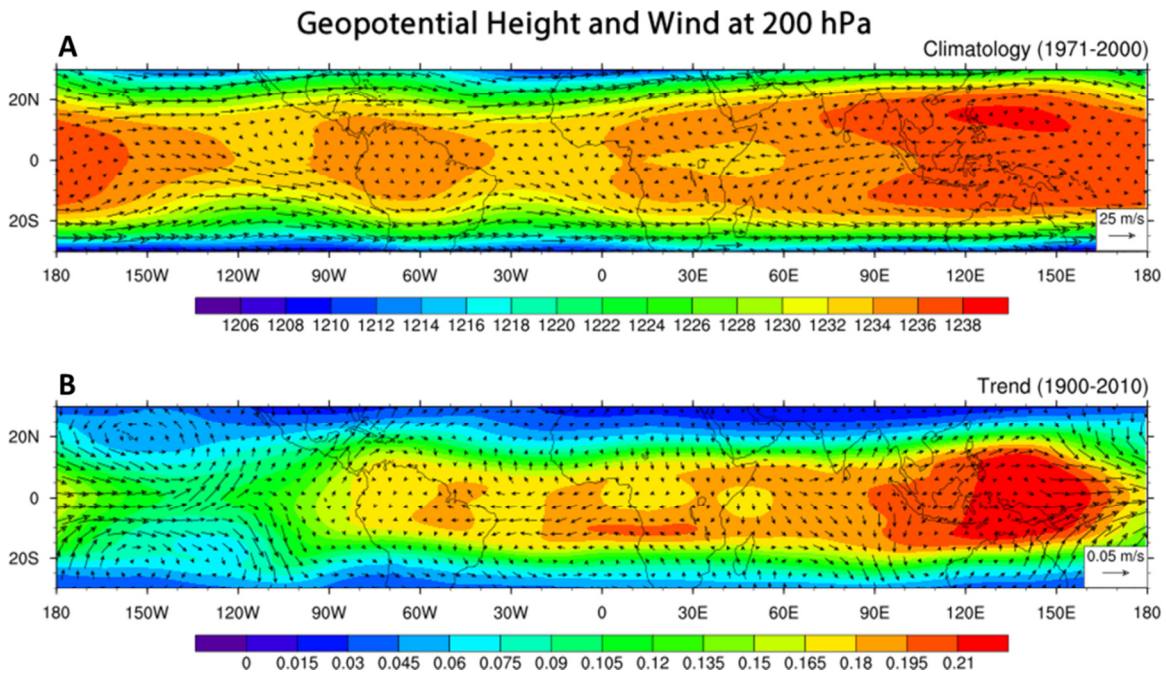
Figure 8: (A) Climatology of the geopotential height (dam) and the wind (m s^{-1}) at 200 hPa; (B) least-squares linear trend of the geopotential height (scaled to dam per decade) and wind (scaled to m s^{-1} per decade) at 200 hPa.

would also lead to increased subsidence and drying in the subtropics. During the dry season (JJA), the northern regional Hadley Cell strengthens and expands considerably. The ascending branch of the northern regional component also shifts southward by approximately 15° latitude (Figs. 3 and 4), forcing the poleward migration of the southern regional component of the Hadley Circulation. The substantial expansion, strengthening, and southward migration of the regional Hadley Circulation over the Amazon during the dry season provides insight into the drying and warming that has occurred in the Amazon forest. The southward migration of the regional Hadley Circulation's ascending branches combined with an increase in regional subsidence would decrease cloud cover over the Amazon forest (15°S–10°N), increase surface warming, and increase evapotranspiration.
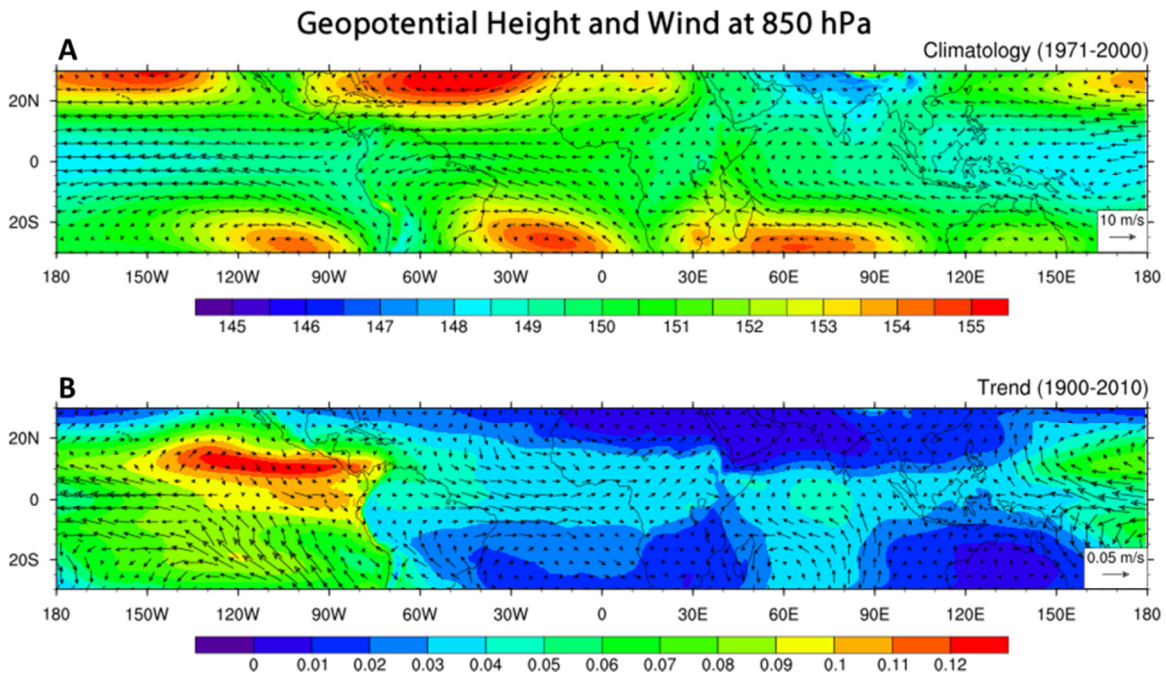
Figure 9:   (A) Climatology of the geopotential height (dam) and the wind (m s^{-1}) at 850 hPa; (B) least-squares linear trend of the geopotential height (scaled to dam per decade) and wind (scaled to m s^{-1} per decade) at 850 hPa.

Essentially, this would mean a more intense dry season. This is further suggested by the emergence of localized seabreeze intensification over northern South America during JJA (Fig. 4) that would form as the temperature difference between the land and sea increased. The regional Hadley Circulation further intensifies over the Amazon during SON, implying that the regional dry-season is prolonged [*Fu et al.,* 2013] as well as intensified.

Over the Congo, the regional Hadley Circulation shows homogenous weakening in the outer tropics/subtropics and slight strengthening of the southern component south of the Congo rainforest (at approximately 10°–20°S) during DJF (Figs. 4 and 5). Furthermore, it appears that the local influence from the Congo forest observed in the climatology (the "tail" of the southern regional component seen in Figure 3) has become

weaker since 1900. The decadal trend (Fig. 5) emphasizes that the climatological "tail" (Fig. 3) has become considerably weaker in the boundary layer over the Congo forest concurrent with a possible southward expansion of the northern regional component and intensification along the equator during DJF. This is reflected in the substantial long-term weakening of the low-level "tail" over the Congo forest (Fig. 5). During MAM, both ascending branches of the regional Hadley Circulation show weakening; however, the descending branch of the northern component in the subtropics has strengthened since 1900. However, there is no discernable trend in the circulation directly over the Congo forest during this season. During JJA, the portion of the southern component of the regional Hadley Circulation that extends into the Northern Hemisphere (Fig. 3) intensifies and deepens between 0°–20°N (Figs. 4 and 5). Between 0°–20° S the southern regional component weakens and subsidence in the subtropics south of 25° strengthens and appears to become more focused in this region. The ascending branch of the northern regional Hadley Cell shifts northward and intensifies during JJA as well (Figs. 4 and 5). During SON, the northern regional Hadley Cell intensifies over the Congo, particularly in the subtropics, and indicates expansion into the mid-latitudes (Figs. 4 and 5). The southern regional Hadley Cell demonstrates strengthening of equatorial ascent and increased subsidence in the subtropics, but also indicates weakening in the lower troposphere between 10°–20° S (just south of the Congo forest). These patterns suggest that regional ascent and subsidence, particularly in the Southern Hemisphere, are becoming more intense, but also becoming more spatially concentrated over the Congo.

3.2 Long-term Changes in Tropical Circulation and Climate

3.2.1 LONG-TERM, ANNUAL TRENDS

Held and Hou [1980] suggested that a warming climate would result in strengthening of the Hadley Circulation due to enhanced rainfall in its rising branch. Lau and Kim [2015] first identified changes in the Hadley Circulation in model simulations that are consistent with this earlier framework in their discovery of the "deep-tropics squeeze" and an overall broadening of the Hadley Circulation due to the anthropogenic greenhouse effect. Later studies have also identified that anthropogenic greenhouse warming results in an expansion of the Hadley Circulation [*Tao et al.,* 2016]. As discussed in Fu [2015], these changes seem to be positively linked to an expanded troposphere and elevated tropopause. Findings in this study support this reasoning. Based on the annual, long-term trend of geopotential height at 200 hPa (Fig. 8B) and 850 hPa (Fig. 9B), it is evident that the height of the tropopause over the tropics is rising, consistent with studies that have identified an intensified warming in the upper troposphere [*Allen and Sherwood*, 2008]. However, it should be noted that the long-term trend does not show uniform warming spatially within the tropics. The increase in the mean temperature of the troposphere is maximized over the Atlantic Ocean, Indian Ocean, and especially the Maritime Continent and Western Pacific. Thus, these are also the regions in which the deepening of the troposphere is maximized.

The annual trends in geopotential heights at 200 hPa (Fig. 8B) and 850 hPa (Fig. 9B) over the eastern Pacific Ocean do not indicate an expansion of the troposphere in this region. A stationary or slight shrinking of the troposphere appears to be related to SST cooling in the eastern Pacific combined with an intensification of the Walker Circulation [*McGregor et al.,* 2014]. An intensification of the Walker Circulation over the Pacific

Trend of Reconstructed Geopotential Height and Wind at 200 hPa

Figure 10:   Seasonal linear trend of the geopotential height (dam per decade) and wind
            (m s^{-1} per decade) at 200 hPa reconstructed from each ocean basin's
            warming mode; only significant trends are shown.

would increase upwelling in the eastern Pacific leading to cooler SSTs in this region.
Strengthening of the Walker Circulation, as further exemplified by the long-term trend in
the zonal winds at 200 hPa (Fig. 8B) and 850 hPa (Fig. 9B), is maximized over the
Maritime Continent and Pacific Ocean. Over the Atlantic Ocean, the Walker Circulation
shows a reversal of the climatology (Figs. 8A and 9A) that favors Atlantic Niño (the
counterpart to El Niño) conditions. This reversal indicates a long-term transition of less
moisture flux entering the Amazon from the Atlantic and more moisture flux from the
Atlantic into the Congo and western Central Africa. This also further supports the
intensified localized seabreezes that were expressed in the long-term trend of the MMSF
over the Amazon (Figs. 4 and 5). As the Walker Circulation reverses, the easterly trade
winds rotate, amplifying meridional movement over northern South America as seen in
Figure 9B. Furthermore, there is substantial strengthening of subtropical high pressure
systems over the Pacific and Indian Oceans related to the intensification of the Walker
Circulation in these regions. Similarly, a long-term weakening of subtropical high

pressure systems is observed in the Atlantic in accordance with the reversal of the Walker Circulation.

3.2.2 SEASONAL ATTRIBUTION TO WARMING OCEAN BASINS

Long-term ocean basin warming in the Pacific, Atlantic and Indian Oceans were analyzed, respectively, to determine the influence of warming in each ocean to forcing long-term, large-scale changes in tropical circulation and climate as well as regional changes in the Amazon and Congo. This was done by using empirical orthogonal functions to extract the long-term warming pattern from each separate ocean basin independently, as detailed in Chapter 2.

Using the statistically significant long-term trends of the reconstructed geopotential heights and winds at 200 hPa (Fig. 10) and 850 hPa (Fig. 11), it is difficult to attribute seasonal, large-scale circulation changes to warming in any individual ocean basin. However, it does appear that warming in the Atlantic Ocean has had the largest influence on the elevation of the tropopause over the Atlantic Ocean, central Africa and South America, the Indian Ocean, and the Maritime Continent year-round (Fig. 10). Warming in the Indian Ocean also significantly influences the elevation of the tropopause in these regions, particularly during MAM, JJA, and SON (Fig. 10). Warming in the Pacific Ocean has the least influence on the elevation of the tropopause, particularly during DJF, but it also appears to have the strongest influence on upper-level winds (Fig. 10). During MAM, JJA, and SON, warming in the Pacific Ocean induces a strengthening of the Hadley Circulation over the Pacific and Maritime Continent, as well as a slight strengthening of the Walker Circulation in the eastern Pacific. Pacific warming also suggests a strengthening of subtropical jets, particularly in the Northern Hemisphere.
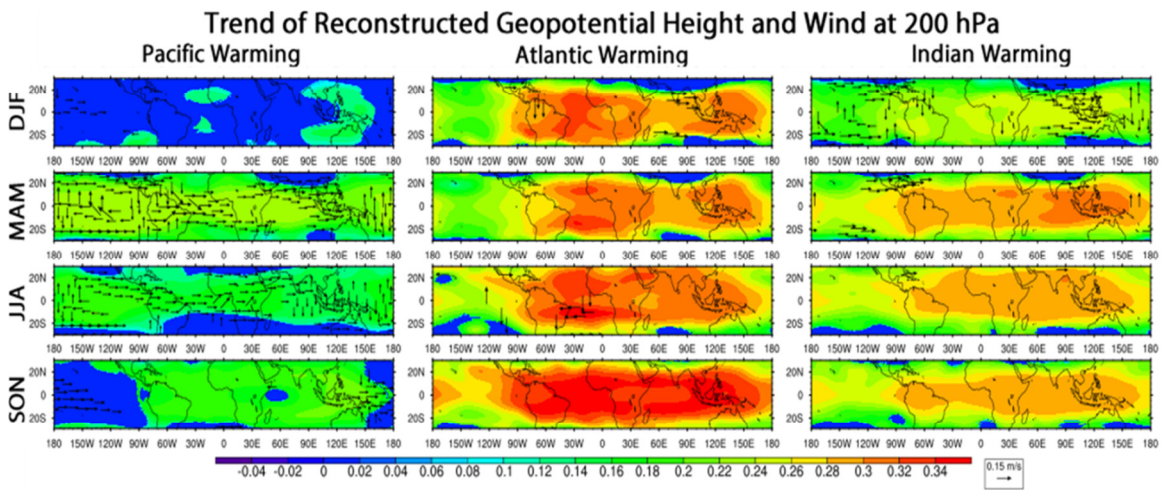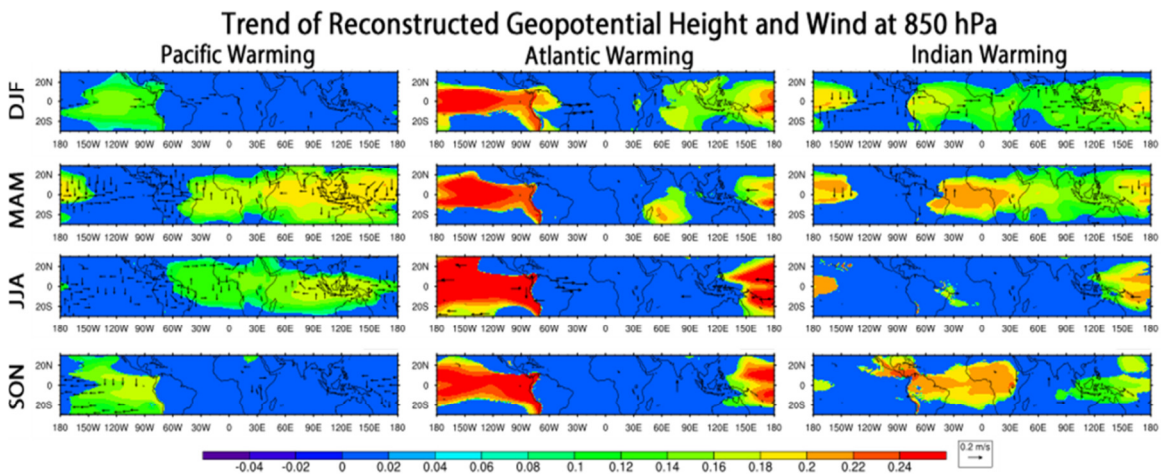
Figure 11:   Seasonal linear trend of the geopotential height (dam per decade) and wind ($m\ s^{-1}$ per decade) at 850 hPa reconstructed from each ocean basin's warming mode; only significant trends are shown.

This is possible as warming SSTs in the Pacific would lead to increased equatorial convection, more divergence aloft, and therefore a stronger subtropical jet. However, warming in the Atlantic Ocean during JJA seems to be the dominant cause of the reversal of the Walker Circulation over the Atlantic Ocean (Fig. 10 and 11). This could be associated with the decrease of precipitation south of 10° S in South America during JJA (Fig. 15) as this would reduce moisture flux into this region of South America from the Atlantic Ocean. This equally could be responsible for the increase in precipitation along the western coast of Africa between 0–10° S during JJA associated with Atlantic Ocean warming (Fig. 19), as will be discussed in more detail shortly.

Ocean basin warming in the Pacific, Atlantic, and Indian Oceans can be attributed to a long-term warming trend in large areas of the Amazon and surrounding lands in South America (Figs. 12–14). Seasonal maximum temperatures have been predominantly increasing along the north coast of South America, the eastern coast, and south of the Amazon (Fig. 12). The Atlantic Ocean appears to have the largest influence on the

33

Figure 12:   Seasonal Theil-Sen trend of the maximum temperature over the Amazon reconstructed from each OBWM scaled to °C per season per decade. Points shown are significant according to the Mann-Kendall trend significance test and show the degree of regional seasonal warming attributable to individual ocean basin warming.

warming in the Amazon seasonally and spatially. However, warming in the Indian Ocean also has a large influence. The Pacific Ocean warming surprisingly has the smallest contribution to warming of maximum temperatures in the Amazon (Fig.12) which most likely reflects the impact the Andes have on climate in the Amazon. From Figure 10, it appeared that Pacific Warming primarily influenced upper-level winds. The Andes could block much of the influence from the Pacific. This would also explain why strengthening

Figure 13: Seasonal Theil-Sen trend of the minimum temperature over the Amazon reconstructed from each OBWM scaled to °C per season per decade. Points shown are significant according to the Mann-Kendall trend significance test and show the degree of regional seasonal warming attributable to individual ocean basin warming.

of the annual Walker Circulation is so strong in the Pacific Ocean but shows weakening across South America (Fig. 9).

Similar to seasonal maximum temperatures, ocean basin warming has led to nearly ubiquitous warming of minimum surface temperatures across the Amazon and South America as well (Fig. 13). Pacific Ocean warming is once again the least influential, whereas Atlantic and Indian Ocean warming are largely influential spatially
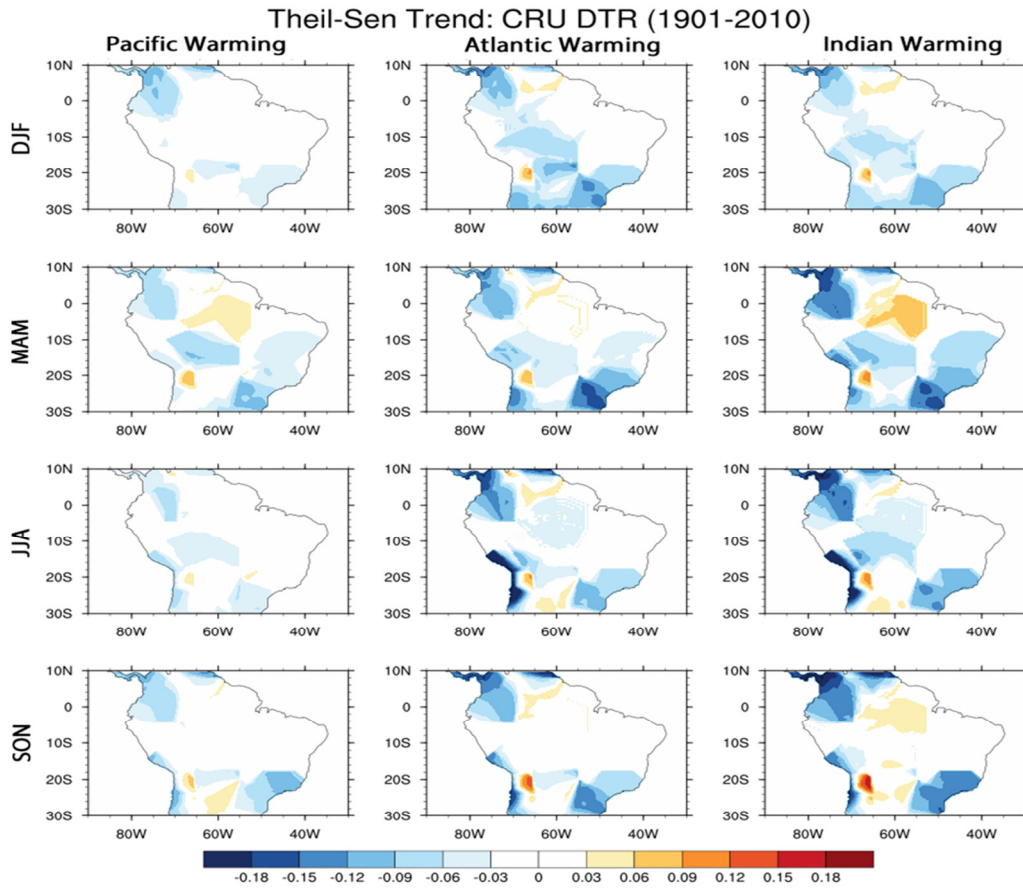
Figure 14:   Seasonal Theil-Sen trend of the diurnal temperature range (DTR) over the Amazon reconstructed from each OBWM scaled to °C per season per decade. Points shown are significant according to the Mann-Kendall trend significance test and show the degree of regional seasonal warming attributable to individual ocean basin warming.

and seasonally. Atlantic warming appears to have a slightly stronger influence on warming of minimum temperatures across the Amazon and South America, but warming in the Indian Ocean appears to be more spatially significant (Fig. 13). It should also be noted that minimum surface temperatures across South America have warmed more than maximum surface temperatures since 1901 as indicated in the reduced diurnal temperature ranges across the region (Fig. 14). The larger increase of minimum surface
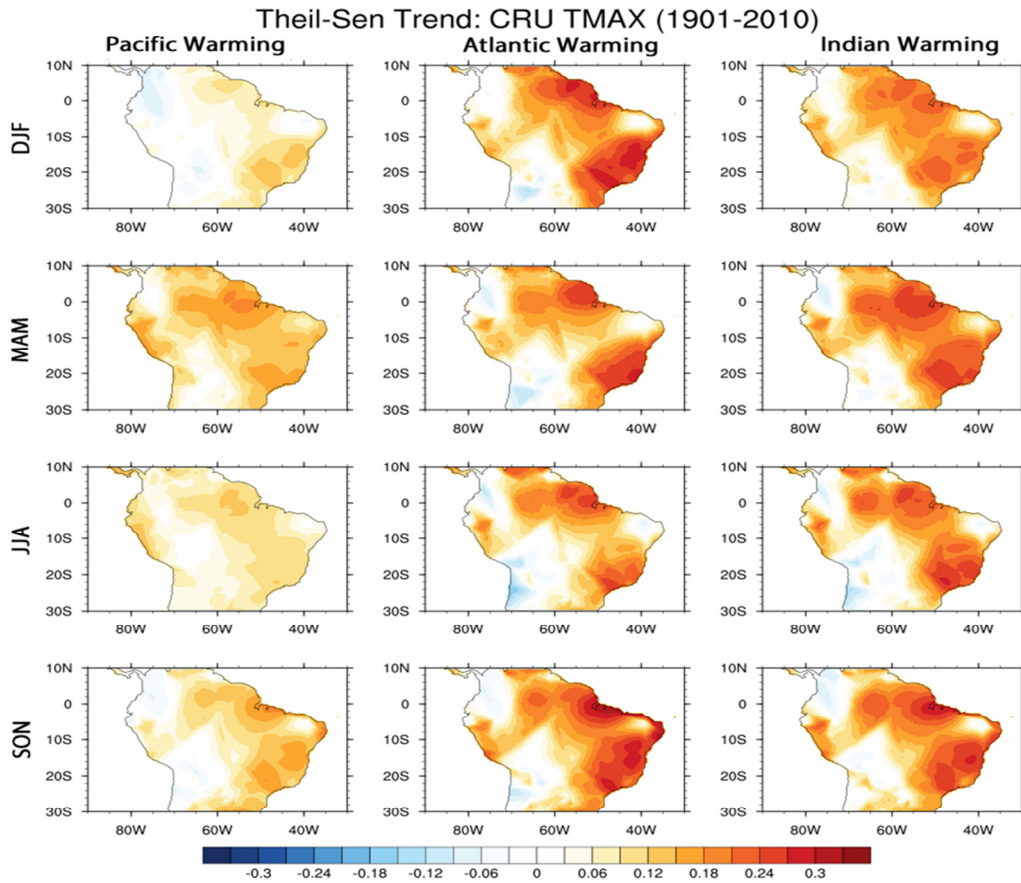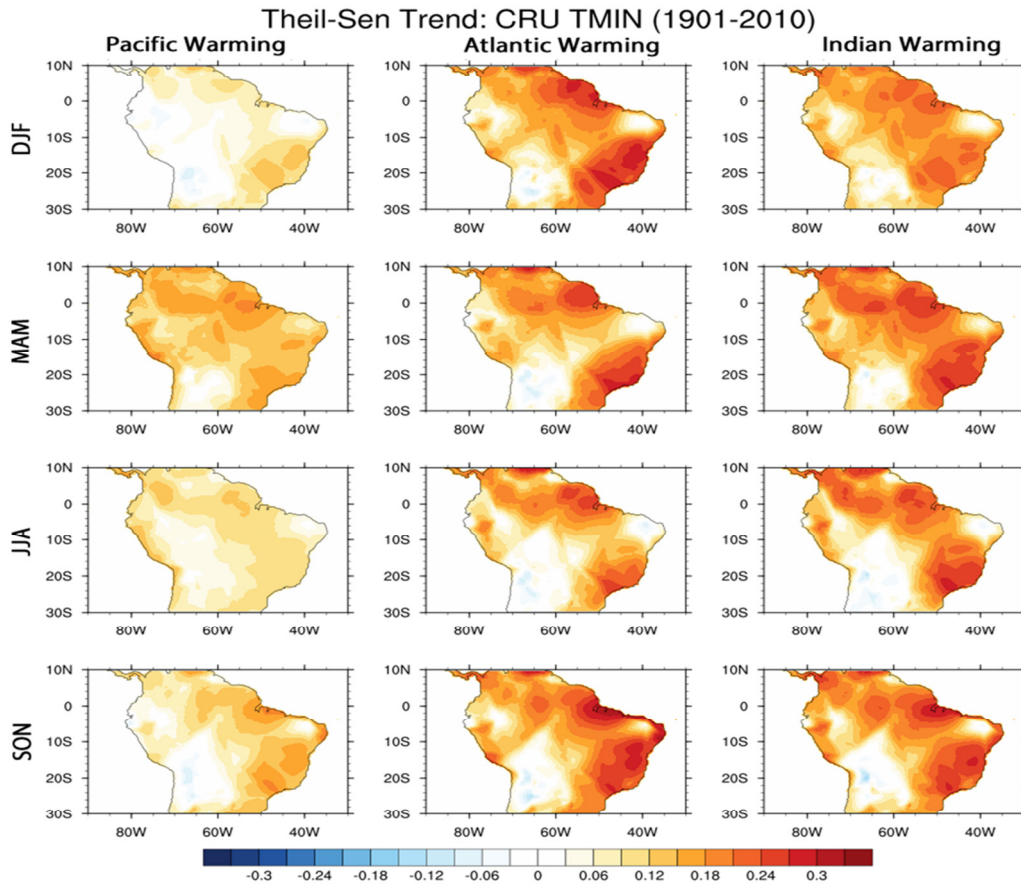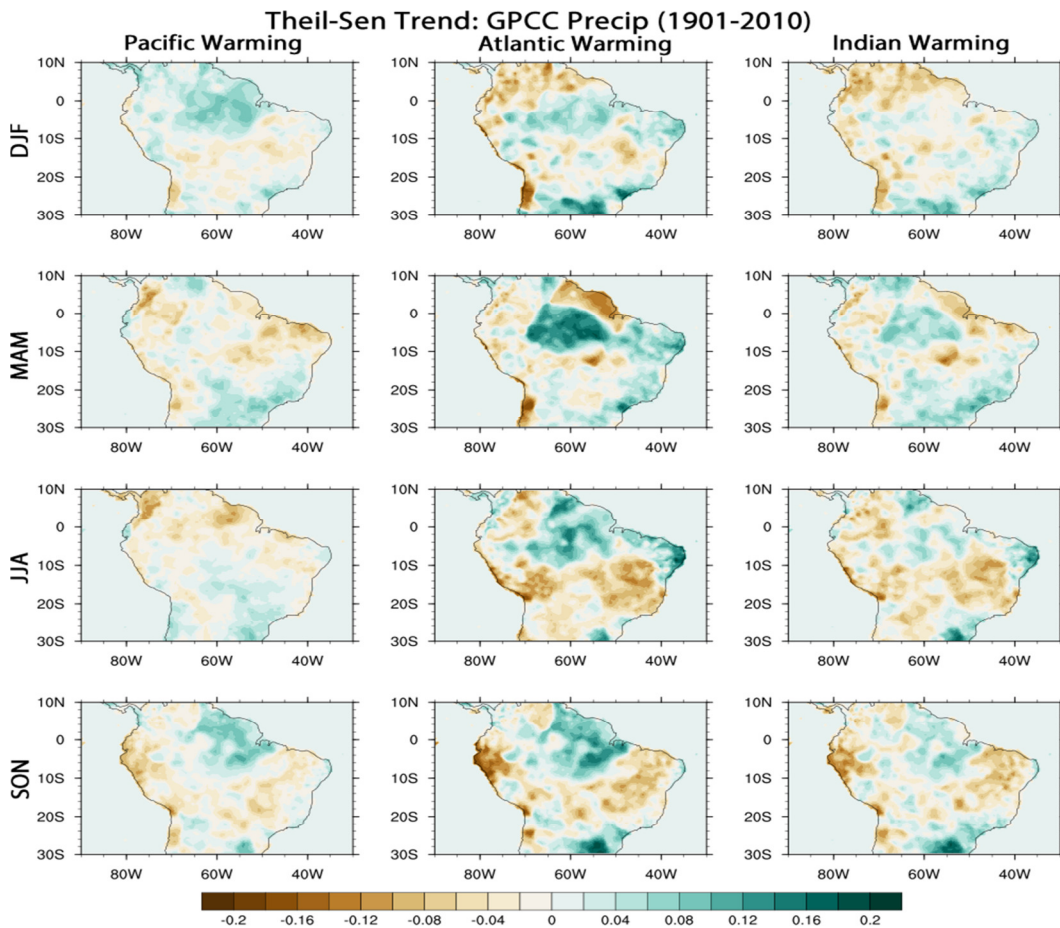
Figure 15: Seasonal Theil-Sen trend of precipitation over the Amazon reconstructed from each OBWM scaled to mm per season per decade. Points shown are significant according to the Mann-Kendall trend significance test and show the degree of regional seasonal precipitation change attributable to individual ocean basin warming.

temperatures in the region could also be attributed to the increase of atmospheric CO_2 or possibly an increase in atmospheric water vapor. As is well-known, a warmer atmosphere promotes more evapotranspiration and can hold more moisture. This would inhibit night-time surface cooling in the region and could promote surface drying as well. The focused warming in both maximum (Fig. 12) and minimum (Fig. 13) surface temperature in northern South America and along the eastern coast across all seasons could also reflect

the reversal of the Walker Circulation seen in Figures 8B and 9B. The long-term trend indicating a reversal of the local Walker Circulation would promote subsidence in these regions which would reduce cloud cover, enhancing diurnal surface warming (maximum temperature). However, it should also be noted that the regions that do show the most statistically significant warming trend are also those encompassing more urbanized areas. The long-term warming could therefore also be attributable to land use changes and urbanization or data bias.

As previously mentioned, the Amazon has experienced several extreme droughts and an overall increase in dry-season length in recent decades [*Marengo et al.*,2011; *Fu et al.*, 2013]. There appears to be no relation to the spatial distribution or magnitude of the long-term warming trends in the Amazon (Figs. 12–14) and the long-term precipitation trends in the Amazon (Fig. 15) other than the minimal influence attributable to Pacific warming. The long-term trends of seasonal precipitation attributable to warming in each ocean basin (Fig. 15) indicate that Atlantic warming has the largest impact on precipitation patterns in the Amazon region. The heart of the Amazon forest appears to have experienced a long-term increase in precipitation across all seasons although the rainy season (DJF) shows the weakest increase. The spatial distribution of the trend for the Atlantic and Indian Oceans are very similar across each season; trends associated with Pacific warming largely oppose those associated with the other two ocean basins in every season except SON. Previous studies have suggested that reduced rainfall in the Amazon is equally attributable to warming SSTs in the Atlantic and the Pacific [*Harris et al.,* 2008]. This discrepancy could be due to the fact that a large portion of tropical Pacific warming was included in the ENSO mode captured by the empirical orthogonal functions methodology. Harris et al. [2008] also suggest that regional strengthening of the South American Monsoon caused by warm Atlantic SSTs is

suppressed by the large-scale atmospheric circulation response to warm Pacific SSTs. This theory is somewhat consistent with findings in this study as Pacific warming was shown to predominantly influence large-scale tropical atmospheric circulation patterns (Figs. 10 and 11).

Reductions in precipitation in the southern Amazon region across all seasons further supports the theory that deforestation and land use changes in this region will reduce local precipitation. Furthermore, the dry season (JJA) and the end of the dry season (SON), show more consistency in the spatial distribution and magnitude of the increase in surface warming (Figs. 12–14) and precipitation trends in the Amazon (Fig. 15). This could indicate that land use changes and aerosols from biomass burning in the southern Amazon during the dry season could be a contributor to localized warming and rainfall reductions. However, this consistency is primarily seen in the trends associated with Atlantic warming which does promote uncertainty in this theory, at least over the long-term. Studies that evaluate changes on a shorter timescale would be better able to deduce the contribution of biomass burning and anthropogenic deforestation on surface temperature and precipitation trends in the Amazon.

Regional surface warming (Figs. 16–18) in the Congo also shows little influence from Pacific warming compared to warming in the Atlantic and Indian Oceans. Long-term trends in maximum surface temperature (Fig. 16) and minimum surface temperature (Fig. 17) are nearly equal for the Atlantic and Indian Oceans. This could be reflective of the lack of large geographical features in the region that would block influences from either bordering ocean basin. Nearly all of central Africa has experienced increased surface warming during the twentieth century during all seasons, consistent with theories on anthropogenic global warming. It should be noted, however, that minimum surface

Figure 16: Seasonal Theil-Sen trend of the maximum temperature over the Congo reconstructed from each OBWM scaled to °C per season per decade. Points shown are significant according to the Mann-Kendall trend significance test and show the degree of regional seasonal warming attributable to individual ocean basin warming.

temperatures are not increasing much more than maximum surface temperatures in the Congo forest (Fig. 18) as was seen in the Amazon (Fig. 14). Surface minimum temperatures appear to be warming equally or slightly less than maximum surface temperatures over the Congo for all seasons and ocean basin warming. However, it is interesting that the deserts surrounding the Congo forest (the Sahara to the north and the Kalahari to the south) are not experiencing consistent temperature changes. Minimum surface temperatures in large portions of the southern Sahara Desert appear to be

Figure 17:   Seasonal Theil-Sen trend of the minimum temperature over the Congo reconstructed from each OBWM scaled to °C per season per decade. Points shown are significant according to the Mann-Kendall trend significance test and show the degree of regional seasonal warming attributable to individual ocean basin warming.

warming faster than maximum surface temperatures in all seasons, consistent across ocean basin warming (Fig. 18). However, equatorial Africa (including the Congo forest) and the Kalahari Desert appear to have experienced amplified diurnal surface warming. This could be due to a weakening and expansion of the regional Hadley Circulation (Figs. 4 and 5). Weaker equatorial convection would reduce local cloud cover over the Congo forest, amplifying diurnal warming. Furthermore, the expansion of the Hadley Circulation would also inhibit cloud cover in the deserts by enlarging regions of
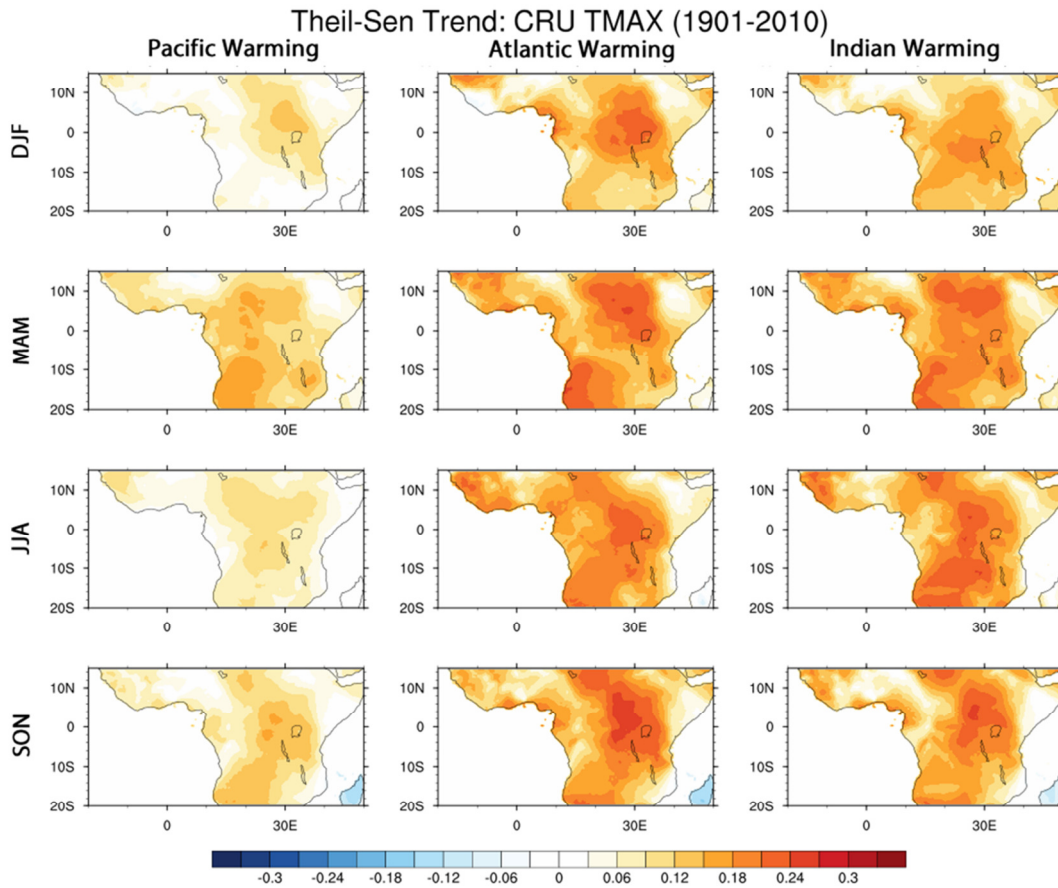
41
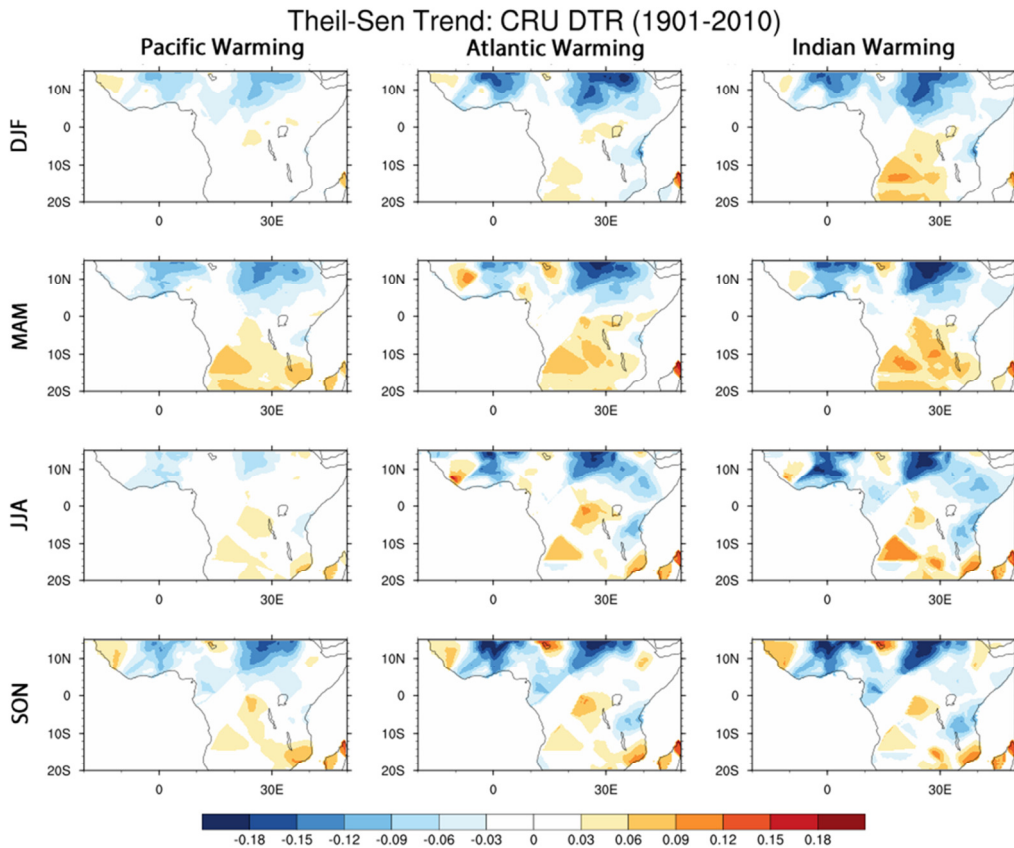
Figure 18: Seasonal Theil-Sen trend of the diurnal temperature range (DTR) over the Congo reconstructed from each OBWM scaled to °C per season per decade. Points shown are significant according to the Mann-Kendall trend significance test and show the degree of regional seasonal warming attributable to individual ocean basin warming.

subsidence. Future work could validate this theory by expanding the analysis into the Sahara Desert to determine if this region also reflects an expansion of the Hadley Circulation. Furthermore, the higher temperatures in tropical Africa could reflect the overall warming of the troposphere, as reflected in Figures 8B and 9B, as tropical African forests are at much higher altitudes than the Amazon [*Otto et al.,* 2013].

Previous studies have associated reduced rainfall in tropical Africa to long-term natural variability in Atlantic SSTs [*Folland et al.,* 1986] and to a lesser extent ENSO
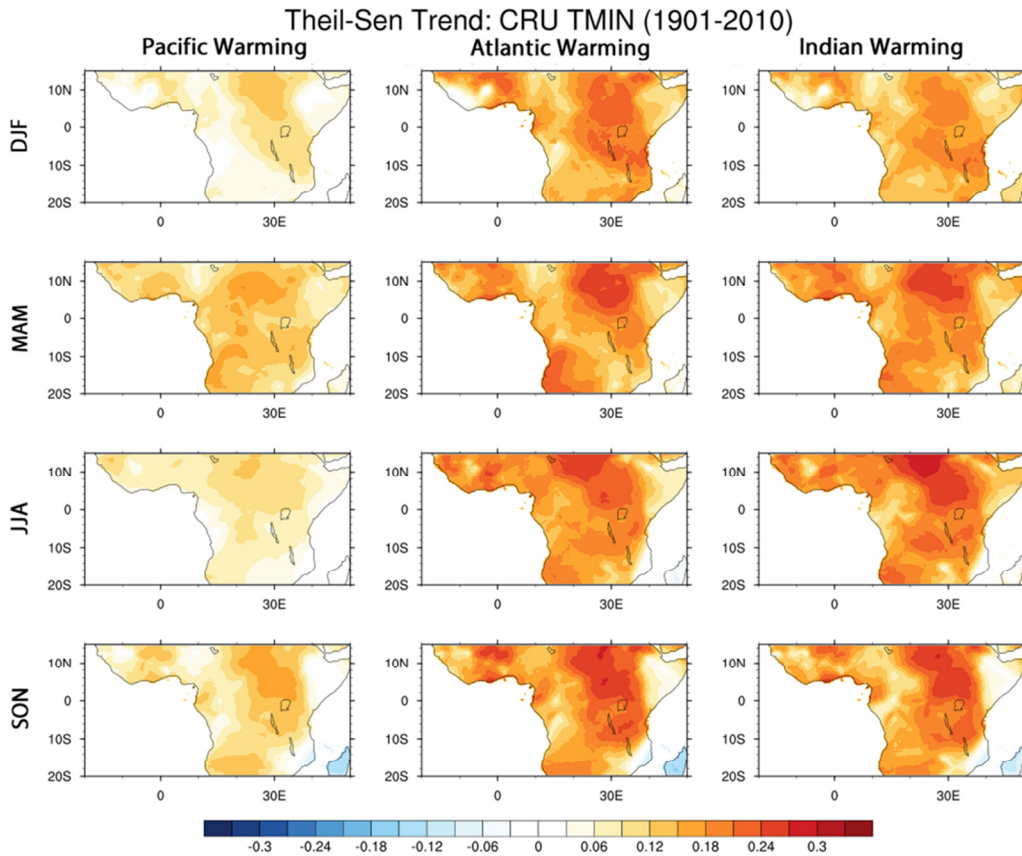
42
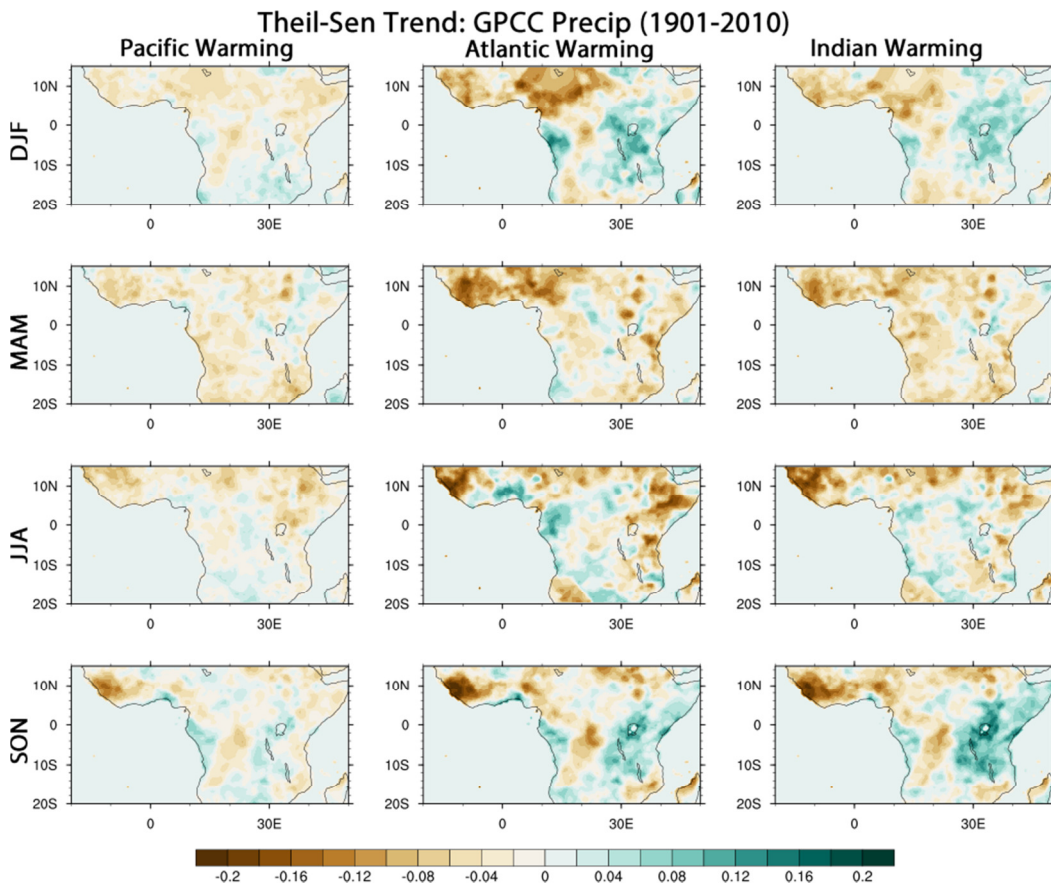
Figure 19:   Seasonal Theil-Sen trend of precipitation over the Congo reconstructed from each OBWM scaled to mm per season per decade. Points shown are significant according to the Mann-Kendall trend significance test and show the degree of regional seasonal precipitation change attributable to individual ocean basin warming.

[*Malhi and Wright*, 2004]. Results from this study indicate substantial drying across large portions of Africa year-round associated with warming tropical SSTs (Fig. 19). Pacific warming appears to reduce precipitation spatially across tropical Africa for all seasons more so than that of Atlantic of Indian warming. However, Pacific warming influences the precipitation trend at a much lower magnitude than the other two ocean basins. Overall, there is much consistency across the long-term, seasonal precipitation trends associated with each ocean basin warming which could indicate that other variables are

responsible these trends. For instance, reduced localized equatorial convection during MAM and JJA (Figs. 4 and 5) could explain the predominant drying trend across equatorial Africa in these seasons (Fig. 19). However, it should be noted that Atlantic warming seems to promote rainfall along the western coast of Africa bordering the Gulf of Guinea. Expansion of the localized descending branches of the Hadley Circulation, particularly in the Southern Hemisphere (Figs. 4 and 5) could be related to the increase of precipitation south of the Congo and into the Kalahari Desert (Fig. 19), as well.

Based on these results, it would appear that tropical Africa is much more vulnerable to extreme droughts than that of tropical South America. Furthermore, the regional similarities between the variable field changes attributable to warming in the Atlantic and Indian Oceans compared to the changes attributable to Pacific Ocean warming suggest that warming across ocean basins may not be uniform. However, the differences may also be due to the large influence that ENSO plays in regional and large-scale climate, as discussed in further detail in the following section.

4. LIMITATIONS AND CONCLUSIONS

4.1 Limitations

Despite the new perspectives this study gives on long-term changes in tropical circulation and climate and their relation to regional changes in the Amazon and Congo tropical forests, there are many limitations of this study. First, using the minimum and maximum values of the MMSF to plot the time series of the strength of the southern and northern Hadley Cells, respectively, may not have captured each respective regional cell over the Amazon or Congo. For instance, over the Amazon the minimum value of the MMSF would have most likely captured the strength of the mid-latitude Ferrel Cell when plotting the annual time series and those for all seasons other than JJA. Furthermore, the strength of either regional cell over the Congo during JJA could have captured features associated with the "mini circulation dome" (Fig. 3) instead of the overall strength of either of the regional Hadley Cells. However, this method does work well for capturing the strength of each respective Hadley Cell for the full tropical belt [*Liu et al.,* 2012].

Using the Theil-Sen trend estimator tested with the Mann-Kendall trend significance test against the reconstructed temperature and precipitation variable fields over the Amazon and Congo (Figs. 12–20) may over-estimate the number of significant data points in these figures. This would occur because the trends are largely based on the OBWM time series (Fig. 2) as described in detail in the Chapter 2. Because the time series for the warming modes are all significantly increasing, the Mann-Kendall trend significance test would reflect this base significance; very few (if any) points would be deemed insignificant. Therefore, it might be beneficial to calculate the linear regression coefficient and test the significance based on the methods described in Chen [1982] and Livezey and Chen [1983] for comparison.

However, the lack of significant data points calculated for the long-term trend in the reconstructed geopotential height and wind data (Figs. 10 and 11) using the methods outlined in Chen [1982] and Livezey and Chen [1983] leave many questions unanswered regarding the role individual ocean basin warming has played in large-scale or regional tropical circulation changes since 1900. It can be deduced that Pacific Ocean warming has a large influence on upper-level winds which is consistent with the established role the Pacific Ocean plays in many large-scale teleconnections. However, contributions to regional climate and circulation changes remain very uncertain. Because of the lack of consistent significant data points, many conclusions based on these results are largely speculative. This lends the question as to if using empirical orthogonal functions is the best methodology to use to extract such long patterns of variance in SSTs, or if using one global ocean warming mode would yield more conclusive results than individual ocean basin warming modes.

4.2 Future Work

An initial first step would be to use the EOF method to extract one global warming mode, one mode representative of ENSO, and possibly one mode for the Atlantic Meridional Overturning Circulation (AMOC). Repeating the analyses performed in this study using these different EOF modes may yield more conclusive results and would provide additional valuable insight as to how these dominant ocean patterns have influenced large-scale and regional changes in tropical circulation and climate. This would help to elucidate changes that have occurred due to anthropogenic greenhouse warming and those that are due to long-term natural variability.

46

An additional next step would include evaluating separate long-term periods. For example, looking at changes prior to 1950 and then after 1950 would enhance the reliability of the results in this study that evaluate overall changes for the twentieth century. Anthropogenic warming has increased dramatically since 1980 [*IPCC,* 2013], and this is also when a significant response of the climate system has been observed in response to long-term anthropogenic warming [*Abram et al.,* 2016]. Furthermore, station data in tropical forests is much more robust after 1950, particularly in the Amazon. Therefore, evaluating time periods from 1951–1980 and 1981–2010 would also be beneficial to better determine the anthropogenic contribution to these changes. As stated earlier, station data is much less consistent and reliable in the Congo tropical forest due to ongoing political unrest, civil conflict, and logistical difficulties. Because of this, it would also be beneficial to apply the methods used in this study to satellite data to deduce how well reanalysis data agrees with satellite data over a shorter time period. This would help to validate the results of the long-term analyses.

Lastly, evaluating long-term trends in regional integrated vapor flux attributable to global ocean warming, ENSO, and AMOC would provide additional insight as to how natural variability and anthropogenic warming have influenced regional drying in the Amazon and Congo tropical forests. Furthermore, by analyzing the long-term changes in the advection of precipitable water over the Amazon and Congo, respectively, as well as the attribution to each EOF ocean, one could better deduce the relative contribution of long-distance teleconnections to regional changes in each tropical forest. This would also further elucidate the relationship of tropical circulation changes to regional climate changes in tropical forests.

47

4.3 Conclusions

The regional and seasonal manifestations of climate change determine the effects of anthropogenic greenhouse warming on ecosystems and society [*Parry et al.*, 2007]. Findings in this study further exemplify the importance of evaluating climate changes in on a regional and seasonal basis by assessing such changes in the Amazon and Congo forests compared to that of the full tropical belt. Results indicate that large-scale atmospheric circulation systems in the tropics have not changed homogenously throughout the tropics.

Based on the results of this study, it can be concluded that the Hadley Circulation has distinct regional manifestations that have not changed uniformly across different regions during the twentieth century and early twenty-first century. Globally, the Hadley Circulation has strengthened in the Southern Hemisphere and weakened in the Northern Hemisphere for the 1900–2010 time period. However, the Hadley Circulation over the Amazon indicates strengthening in both hemispheres and weakening in both hemispheres over the Congo. A strengthening of the Walker Circulation has also been identified in the Pacific and Atlantic Oceans and over the Maritime Continent. However, long-term changes of the Walker Circulation over the Atlantic are indicative to Atlantic Niño (the Atlantic counterpart of the El Niño) conditions, as represented in substantial reversals of climatological zonal wind patterns. These wind reversals indicate less moisture influx into the Amazon from the Atlantic Ocean and more moisture influx into the Congo from the Atlantic. However, long-term, seasonal precipitation trends indicate that the Congo has experienced more extreme drying than the Amazon due to ocean basin warming.

Long-term changes in the Hadley Circulation over the full tropical belt validate previous studies that suggest a narrowing and deepening of equatorial convection,

enhanced uplift, and an expansion of the descending branches of the Hadley Circulation into the tropics and subtropics as a result of anthropogenic warming [*Lau and Kim*, 2015]. The "deep tropics squeeze" seen across all seasons in the long-term trend of the Hadley Circulation over the full tropics supports the theory that anthropogenic warming is very influential on tropical atmospheric circulation, as was seen in CMIP5 models evaluated by Lau and Kim [2015]. Furthermore, results from this study agree with similar evaluations of the Hadley Circulation throughout the twentieth century that used a different twentieth century reanalysis dataset. This further validates the results of this study as well as exemplifies consistency among twentieth century reanalysis datasets.

Although findings from this study agree with previous studies that link anthropogenic warming to changes tropical atmospheric circulation, attribution analyses in this study are much less conclusive. This study did find that anthropogenic warming is expanding the depth of the troposphere in the tropics, although this is occurring unevenly. Additionally, warming in the Pacific Basin was found to have the greatest influence on upper-level circulation in the tropics. Overall however, using ocean basin warming modes to deduce the contribution to long-term changes in tropical circulation and particularly regional climate changes in the Amazon and Congo does not illicit very conclusive results. This acknowledges the limitations of using empirical orthogonal functions to attribute long-term atmospheric circulation and regional climate changes to ocean warming. Conversely, although the results do suggest that warming across different ocean basins may not be occurring homogenously, repeating this analysis with one global ocean warming mode would still be beneficial.

Overall, these findings provide valuable insight into how interactions between oceans and atmospheric circulation systems influence regional climate in the Amazon and Congo. The annual, long-term trends identified in this study provide additional

support for strengthening of the Hadley Circulation proposed by Held and Hou [1980] and help to validate the deep-tropics squeeze identified in Lau and Kim [2015]. These findings will help to improve climate projections in the tropics by providing an essential foundation of seasonal and regional manifestations of tropical atmospheric circulation systems and how long-term changes in these systems have influenced climate in the Amazon and the Congo forests.

Works Cited

Abram, N. J., H. V. McGregor, J. E. Tierney, M. N. Evans, N. P. McKay, D. S. Kaufman, and the PAGES 2k Consortium (2016), Early onset of industrial-era warming across the oceans and continents, *Nature*, *536*, 411-418, doi: 10.1038/nature19082.

Adger, W. N., S. Huq, K. Brown, D. Conway, M. Hulme (2003), Adaptation to climate change in the developing world, *Prog. Devel. Studies, 3,* 179-195, doi: 10.1191/1464993403ps060oa.

Allen, R. J. and S. C. Sherwood (2008), Warming maximum in the tropical upper troposphere deduced from thermal winds, *Nat. Geosci.,1*, 399-403, doi: 10.1038/ngeo208.

Asefi-Najafabady S., and S. Saatchi (2013), Response of African humid tropical forests to recent rainfall anomalies. *Phil. Trans. R. Soc. B*, *368*, 20120306, doi: 10.1098/rstb.2012.0306.

Becker, A., P. Finger, A. Meyer-Christoffer, B. Rudolf, K. Schamm, U. Schneider, and M. Ziese (2013), A description of the global land-surface precipitation data products of the Global Precipitation Climatology Centre with sample applications including centennial (trend) analysis from 1901-present, *Earth Syst. Sci. Data*, *5*(1), 71–99, doi: 10.5194/essd-5-71-2013.

Betts, R. A., Y. Malhi, and J. T. Roberts (2008), The future of the Amazon: new perspectives from climate, ecosystem and social sciences, *Philos. Trans. R. Soc. Lond. B. Biol. Sci.*, *363*(1498), 1729-1735, doi: 10.1098/rstb.2008.0011.

Bonan, G.B. (2008), Forests and climate change: Forcings, feedbacks, and the climate benefits of forests, *Science*, *320*(5882), 1444-1449, doi: 10.1126/science.1155121.

Brienen, R. J. W., et al. (2015), Long-term decline of the Amazon carbon sink, *Nature*, *519*, 344-348, doi:10.1038/nature14283.

Carson, J. F., B. S. Whitney, F. E. Mayle, J. Iriarte, H. Prumers, J. D. Soto, and J. Watling (2014), Environmental impact of geometric earthwork construction in pre-Columbian Amazonia, *Proc. Natl. Acad. Sci. USA, 111*(29), 10497-10502, doi: 10.1073/pnas.1321770111.

Chen, W. Y. (1982), Fluctuations in Northern Hemisphere 700 mb height field associated with the Southern Oscillation, *Mon. Wea. Rev., 110*, 808-823.

Clark, D. A. (2004), Sources or sinks? The responses of tropical forests to current and future climate and atmospheric composition, *Philos. Trans. R. Soc. Lond. B. Biol. Sci.*, *359*(1443), 477-491, doi: 10.1098/rstb.2003.1426.

Cusack, D. F., J. Karpman, D. Ashdown, Q. Cao, M. Ciochina, S. Halterman, S. Lydon, and A. Neupane (2016), Global change effects on humid tropical forests:

Evidence for biogeochemical and biodiversity shifts at an ecosystem scale, *Rev. Geophys.*, *54*(3), 523–610, doi:10.1002/2015RG000510.

Dima, I. M. and J. M. Wallace (2003), On the seasonality of the Hadley Cell, *Journ. Atmos. Sci., 60*, 1522-1527, doi: 10.1175/1520-0469.

Folland, C. K., T. N. Palmer, and D. E. Parker (1986), Sahel rainfall and worldwide sea temperatures, 1901–1985, *Nature, 320*, 602–607, doi:10.1038/320602a0.

Fu, R. (2015) Global warming-accelerated drying in the tropics, *Proc Natl Acad Sci USA, 112*, 3593–3594, doi: 10.1073/pnas.1503231112.

Fu, R., et al. (2013), Increased dry-season length over southern Amazonia in recent decades and its implication for future climate projection, *Proc. Natl. Acad. Sci. USA*, *110*(45), 18110–18115, doi: 10.1073/pnas.1302584110.

Harris, P. P., C. Huntingford, and P. M. Cox (2008), Amazon Basin climate under global warming: the role of the sea surface temperature, *Phil. Trans. R. Soc. B*, *363*, 1753–1759, doi:10.1098/rstb.2007.0037.

Harris, I., P. D. Jones, T. J. Osborn, and D. H. Lister (2014), Updated high-resolution grids of monthly climatic observations—The CRU TS3.10 Dataset, *Int. J. Climatol., 34*, 623–642, doi:10.1002/joc.3711.

Hausfather, Z., K. Cowtan, D. C. Clarke, P. Jacobs, M. Richardson, and R. Rohde (2017), Assessing recent warming using instrumentally homogenous sea surface temperature records. *Sci. Adv., 3*(1), e1601207, doi: 10.1126/sciadv.1601207.

He, J., and B. J. Soden (2015), Anthropogenic weakening of the tropical circulation: The relative roles of direct CO2 forcing and sea surface temperature change, *J. Clim., 28*(22), 8728-8742, doi: 10.1175/jcli-d-15-0205.1.

Held, I. M. and A. Y. Hou (1980), Nonlinear axially symmetric circulations in a nearly inviscid atmosphere. *J. Atmos. Sci., 37*(3), 515–533.

Hersbach, H., C. Peubey, A. Simmons, P. Berrisford, P. Poli, and D. Dee (2013), ERA-20CM: A twentieth-century atmospheric model ensemble. *Q.J.R. Meteorol. Soc, 141*, 2350–2375. doi:10.1002/qj.2528.

Hilker, T., A. I. Lyapustin, C. J. Tucker, F. G. Hall, R. B. Myneni, Y. Wang, J. Bi, Y. M. de Moura, and P. J. Sellers (2014), Vegetation dynamics and rainfall sensitivity of the Amazon, *Proc. Natl. Acad. Sci. USA*, *111*(45), 16041-16046, doi: 10.1073/pnas.1404870111.

Hodell, D. A., J. H. Curtis, and M. Brenner (1995), Possible role of climate in the collapse of Classic Mayan civilization, *Nature, 375*, 391-394.

Horel, J. D. and J. M. Wallace (1981), Planetary-scale atmospheric phenomena associated with the Southern Oscillation. *Mon. Weath. Rev., 109*, 813–829.

Hu, Y. and Q. Fu (2007), Observed poleward expansion of the Hadley circulation since 1979, *Atmos. Chem. Phys., 7*, 5229–5236, doi:10.5194/acp-7-5229-2007.

Huang, B., V. F. Banzon, E. Freeman, J. Lawrimore, W. Liu, T. C. Peterson, T. M. Smith, P. W. Thorne, S. D. Woodruff, and H.-M. Zhang (2015), Extended reconstructed sea surface temperature version 4 (ERSST. v4). Part I: Upgrades and intercomparisons, *J. Clim., 28*(3), 911–930.

IPCC (2013), *Climate Change 2013: The Physical Science Basis. Contribution of Working Group I to the Fifth Assessment Report of the Intergovernmental Panel on Climate Change*, edited by T. F. Stocker et al., pp. 1535, Cambridge Univ. Press, Cambridge, U. K. [Available at http://www.climatechange2013.org/report/full-report/ipcc.]

Juarez, R. I. N., W. Li, R. Fu, and K. Fernandes (2009), Comparison of precipitation datasets over the tropical South American and African continents, *J. Hydrometeorol., 10*, 289-299, doi: 10.1175/2008JHM1023.1.

Lau, W. K. M. and K. M. Kim (2015), Robust Hadley Circulation changes and increasing global dryness due to CO2 warming from CMIP5 model projections, *Proc Natl Acad Sci USA, 112* (12), 3630-3635, doi: 10.1073/pnas.1418682112.

Levitus, S., et al. (2012), World ocean heat content and thermosteric sea level change (0-2000 m), 1955-2010, *Geophys. Res. Lett.*, *39*, L10603, doi: 10.1029/2012GL051106.

Lewis, S. L., P. M. Brando, O. L. Phillips, G. M. F. van der Heijden, and D. Nepstad (2011), The 2010 Amazon drought, *Science*, *331*, 554, doi: 10.1126/science.1200807.

Liu, J., M. Song, Y. Hu, and X. Ren (2012), Changes in the strength and width of the Hadley Circulation since 1871, *Clim. Past*, *8*, 1169-1175, doi:10.5194/cp-8-1169-2012.

Livezey, R. E. and W. Y. Chen (1983), Statistical field techniques and its determination by Monte Carlo techniques, *Mon. Wea. Rev., 111*, 46-59.

Lorenz, E. N. (1956), *Empirical orthogonal functions and statistical weather prediction*, Scientific Report 1, Statistical Forecasting Project, MIT, Department of Meteorology, Cambridge, Mass, USA.

Marengo, J. A., C. A. Nobre, J. Tomasella, M. D. Oyama, G. S. de Oliveira, R. de Oliveira, H. Camargo, L. M. Alves, and I. F. Brown (2008), The drought of Amazonia in 2005, *J. Clim., 21*(3), 495-516, doi: 10.1175/2007JCLI1600.1.

Marengo, J. A., J. Tomasella, L. M. Alves, W. R. Soares, and D. A. Rodriguez (2011), The drought of 2010 in the context of historical droughts in the Amazon region, *Geophys. Res. Lett.*, *38,* L12703, doi: 10.1029/2011GL047436.

Marshall, J., J. R. Scott, K. C. Armour, J.-M. Campin, M. Kelley, and A. Romanou (2015), The ocean's role in the transient response of climate to abrupt greenhouse gas forcing, *Clim. Dyn.*, *44*(7), 2287-2299, doi: 10.1007/s00382-014-2308-0.

Malhi, Y., J. T. Roberts, R. A. Betts, T. J. Killeen, W. Li, and C. A. Nobre (2008), Climate change, deforestation, and the fate of the Amazon, *Science*, *319*(5860), 169-172, doi: 10.1126/science.1146961.

Malhi, Y. and J. Wright (2004), Spatial patterns and recent trends in the climate of tropical rainforest regions, *Phil. Trans. R. Soc. Lond. B., 359*, 311–329, doi: 10.1098/rstb.2003.1433.

Malhi, Y., S. Adu-Bredu, R. A. Asare, S. L. Lewis, and P. Mayaux (2013), African rainforests: past, present and future, *Phil. Trans. R. Soc. B*, *368*(1625), 20120312, doi: 10.1098/rstb.2012.0312.

McGregor, S., A. Timmermann, M. F. Stuecker, M. H. England, M. Merrifield, F. F. Jin, and Y. Chikamoto (2014), Recent Walker circulation strengthening and Pacific cooling amplified by Atlantic warming, *Nature Clim. Change, 4*(10), 888-892, doi: 10.1038/nclimate2330.

Mertz, O., K. Halsnaes, J. E. Olesen, and K. Rasmussen (2009), Adaptation to climate change in developing countries, *Environ. Manage., 43,* pp. 743-752, doi:10.1007/s00267-008-9259-3.

Morton, D. C., R. S. DeFries, Y. E. Shimabukuro, L. O. Anderson, E. Arai, F. del Bon Espirito-Santo, R. Freitas, and J. Morisette (2006), Cropland expansion changes deforestation dynamics in the southern Brazilian Amazon. *Proc. Natl. Acad. Sci. USA*, *103*(39), 14637–14641, doi: 10.1073/pnas.0606377103.

Neukom, R., et al. (2014), Inter-hemispheric temperature variability over the past millennium, *Nat. Clim. Chang.*, *4*(5), 362-367, doi: 10.1038/NCLIMATE2174.

Nogherotto, R., E. Coppola, F. Giorgi, and L. Mariotti (2013), Impact of Congo Basin deforestation on the African Monsoon, *Atmo. Sci. Let., 14*(1), 45-51, doi: 10.1002/asl2.416.

Oslisly, R., L. White, I. Bentaleb, C. Favier, M. Fontugne, J. Gillet, and D. Sebag (2013), Climatic and cultural changes in the west Congo Basin forests over the past 5000 years, *Philos. Trans. R. Soc. B, 368*, 20120304, doi:/10.1098/rstb.2012.0304.

Otto, F. E. L., R. G. Jones, K. Halladay, and M. R. Allen (2013), Attribution of changes in precipitation patterns in African rainforests, *Phil Trans R Soc B, 368*, 20120299, doi: 10.1098/rstb.2012.0299.

Pan, Y., et al. (2011), A large and persistent carbon sink in the world's forests, *Science*, *333*(6045), 988–993, doi: 10.1126/science.1201609.

Phillips, O. L., et al. (2009), Drought sensitivity of the Amazon rainforest, *Science*, *323*, 1344-1347, doi: 10.1126/science.1164033.

Rudolf, B. and U. Schneider (2005), Calculation of gridded precipitation data for the global land-surface using in-situ gauge observations, in *Proceedings of the 2nd Workshop of the International Precipitation Working Group*, pp. 231–247, Global Precipitation Climatology Centre, Germany.

Schneider U., A. Becker, P. Finger, A. Meyer-Christoffer, B. Rudolf, and M. Ziese (2011), GPCC Full Data Reanalysis Version 6.0 at 0.5°: Monthly Land-Surface Precipitation from Rain-Gauges Built on GTS-based and Historic Data, doi: 10.5676/DWD_GPCC/FD_M_V6_050.

Schneider U, A. Becker, P. Finger, A. Meyer-Christoffer, M. Ziese, and B. Rudolf (2014), GPCC's new land surface precipitation climatology based on quality-controlled in situ data and its role in quantifying the global water cycle. *Theor. Appl. Climatol. 115*, 15–40, doi: 10.1007/s00704-013-0860-x.

Soares, D., H. Lee, P. C. Loikith, A. Barkhordarian, and C. R. Mechoso (2016), Can significant trends be detected in surface air temperature and precipitation over South America in recent decades?, *Int. J. Climatol.*, *37*, 1483-1493, doi: 10.1002/joc.4792.

Tao, L., Y. Hu, and J. Liu (2016), Anthropogenic forcing on the Hadley Circulation in CMIP5 simulations, *Clim. Dyn., 46*, 3337-3350, doi: 10.1007/s00382-015-2772-1.

Webster, P. J. (2004), The elementary Hadley Circulation, in *The Hadley Circulation: Present, Past, and Future*, edited by H. F. Diaz and R. S. Bradley, pp. 6-60, Kluwer Academic Publishers, Dordrecht, The Netherlands.

Werth, D. and R. Avissar (2002), The local and global effects of Amazon deforestation, *J. Geophy. Res.*, *107*(D20), 8087, doi: 10.1029/2001JD000717.

Wilcox, R. R. (2012), Introduction to Robust Estimation and Hypothesis Testing, Academic Press, San Diego, Calif.

Winter, A., et al. (2015), Persistent drying in the tropics linked to natural forcing, *Nat. Comm., 6* (7627), 1-8, doi: 10.1038/ncomms8627.

Zhang, X., F.W. Zwiers, G. C. Hegerl, F. H. Lambert, N. P. Gillet, S. Solomon, P. A. Stott, and T. Nozawa (2007), Detection of human influence on twentieth-century precipitation trends, *Nature*, *448*, 461-465, doi: 10.1038/nature06025.

Zhou, L. et al. (2014), Widespread decline of Congo rainforest greenness in the past decade, *Nature, 509*, 86-90, doi:10.1038/nature13265.